Supporting Information for

Metal-organic framework derived CuO catalysts for efficient hydrogenolysis of hardwood lignin into phenolic monomers

Qian Xu, Qiang Wang, Ling-Ping Xiao*, Xiao-Ying Li, Xi Xiao, Meng-Xin Li, Meng-Ran Lin, Yu-Man Zhao and Run-Cang Sun*

Liaoning Key Lab of Lignocellulose Chemistry and BioMaterials, Liaoning Collaborative Innovation Center for Lignocellulosic Biorefinery, College of Light Industry and Chemical Engineering, Dalian Polytechnic University, Dalian 116034, China

* Corresponding authors.

E-mail addresses: lpxiao@dlpu.edu.cn (L.-P. Xiao); rsun3@dlpu.edu.cn (R.-C. Sun).

Table of Contents

1. General Information

Materials

All commercially available compounds were used as received, unless otherwise noted. Methanol and *p*-phthalic acid (H_2BDC) were purchased from Aladdin. Zirconium (IV) chloride and N, N-Dimethylformamide (DMF) were purchased from Energy Chemical. Commercial cellulase (Cellic@ CTec2, 100 FPU/mL) and hemicellulase (shearzyme 500 L, 100,000 IU/mL) were kindly provided from Novozymes (Beijing, China). $CuAc_2 \cdot H_2O$ (99.0%) was purchased from Macklin. Commercially available Pd/C (5 wt%) and Ru/C (5 wt%) were purchased from Aladdin. Methanol and 1,3,5-Benzenetricarboxylic acid were purchased from Energy Chemical, China. All commercially available chemical reagents were used without further unification unless especially noted. Poplar (5 years old), beech (5 years old), birch (*Betula alnoides*, 6 years old), and eucalyptus (*Eucalyptus robusta*, 5 years old) were used as raw materials were employed in this paper, which were extracted, crushed and screened into powders in size of 40 ~ 60 meshes (0.5 ~ 1.0 mm), and dried vacuum at 50 °C for 72 h before used. Lignin models and polymeric lignin model were synthesized according literatures.[1,2] Dimeric and polymeric lignin model compounds were prepared following the literature reports.[3,4]

Equipment and Methods

The Brunauer-Emmett-Teller (BET) surface area computed by multipoint BET analysis of N_2 adsorption constant temperature line and N_2 adsorption–desorption constant temperature line was performed using a Kubo-X1000 equipment (Beijing Builder Co. Ltd, China) by liquid N_2 (-196 °C). Samples were allowed to degas under vacuum prior to measurement for 5 h at 300 °C. X-ray diffraction (XRD) analysis was performed on a Shimadzu Lab XRD-6100 diffractometer with a Cu Kα radiation source operating at 15 mA with 40 kV. Samples have been swept from 10° to 70° (2θ) at 5° min^{-1}. X-ray photoelectron spectra (XPS) was obtained using scanning X-ray microprobe (PHI 5000 Verasa, ULAC-PHI, Inc.) with AI Ka emission and 284.80 eV C1s peak used for an internal standard. After catalyst samples were dissolved in HF solution, the Cu and Zr content was measured through inductively coupled plasma

atomic emission spectroscopy (ICP-AES) using the Thermos IRIS Intrepid II XSP emission spectroscopy. Thermogravimetric analysis (TGA) was carried out at room temperature under a heating rate of 10 °C/min until 800 °C and a N_2 flow rate of 40 mL/min. Transmission electron microscope (TEM) was performed by a JEM-2100F FETEM fitted with energy dispersive X-ray spectrometer (EDX) for analysis at 100 kV, and the high-angle annular dark-field scanning TEM (HAADF-STEM). EDX elemental mapping was carried out at 200 kV. The NH_3-TPD was tested on Micromeritics AutoChem II 2920 apparatus to determine the number of acid sites. Typically, about 100 mg of catalyst was restored in the H_2 stream at 200 ^oC over 60 min, and before being cooled down to room temperature in the He stream. NH_3-TPD was allowed to increase in temperature from 50 ^oC to 650 ^oC at 10 °C min^{-1} for 30 min. CO_2-TPD assays were made on Micromeritics Autochem 2920 apparatus. A sample was restored at 300 ^oC then purged for 1 h in a 10% H_2/Ar stream, and chilled to 50 ^oC in a He flow. After being exposed to a 5% CO_2/He flows (1 h; 50 ^oC) and purged with He (1 h; 50 ^oC), the sample was treated to 500 ^oC at 5 °C min^{-1} at a 30 cm min^{-1} He streams, and the dehydrogenated gas was examined by TCD.

Nuclear magnetic resonance (NMR) spectra were obtained on a Bruker Ascend-400 MHz spectrometer.[5] Samples of lignin (~ 60 mg) were added to 0.55 mL of DMSO-d_6 and 0.14 mL of pyridine, then ultrasonication until solids dissolved. Samples of lignin oil (~ 60 mg) were solubilized in DMSO-d_6. As for ^{13}C-^1H heteronuclear singular quantum correlation nuclear magnetic resonance (2D HSQC NMR), the centrical (DMSO-d_6) peak was used at δ_C/δ_H 39.5/2.49 ppm as an internal reference.

2. Synthesis of CuO/collapse-UiO-66 (abbreviated as CuO/c-UiO-66) catalyst

Synthesis of UiO-66

UiO-66 was synthesized by a hydrothermal synthesis with a minor modification according to previous report.[6] Concisely, 0.9342 g of $ZrCl_4$ and 0.6651 g of H_2BDC were dissolved into 80 mL DMF by ultrasound for 20 min. The obtained mixture was then transferred into a reactor and heated at 120 ^oC for 24 h. The white powder was obtained by centrifugation and washed several times with methanol, and then put in an oven overnight at 60 ^oC.

Synthesis of CuO/c-UiO-66

0.2508 g UiO-66 was added into 50 mL methanol with ultrasound for 30 min. Subsequently, 0.2397 g $CuAc_2 \cdot H_2O$ was mixed into the above suspension followed by a 1 h of magnetic stirring at room temperature. After that, $NaBH_4$/MeOH solution [$NaBH_4$: methanol = 1.45 mg mL^{-1}, $n(NaBH_4) = 5n(Cu^{2+})$] was immediately added to the above dispersion and kept for 2.5 h. The precipitate was collected by filtration and washed several times with methanol, and then dried at 60 ^oC overnight. Finally, the product was calcined in air at 400 ^oC for 2 h with a heating rate of 2 ^oC min^{-1}. The obtained product was denoted as CuO/c-UiO-66.

Synthesis of CuO

An appropriate amount of $CuAc_2$-H_2O was dissolved in 50 mL of methanol, then $NaBH_4$/MeOH solution (as described above) was added to the above dispersion and mechanically stirred for 2.5 h. Finally, it was calcined at 400 ^oC for 2 h. The product obtained was donated as CuO.

Synthesis of ZrO_2

2 g of $ZrCl_4$ was dissolved in 50 mL of 2-propanol and then 5 mL of H_2O_2 solution (30% v/v) was added dropwise while stirring. Adding 2M ammonium solution to the above solution to adjust pH = 9 and stirred for 48 h. The solid was filtered under an ultrasonic irradiation probe for 30 min and dried in an oven at 60 °C overnight. white ZrO_2 powder was obtained by calcinating at 500 °C for 3 h.

3. Characterization of CuO/c-UiO-66

Table S1. ICP-AES analyses for the fresh CuO/c-UiO-66 and spent catalysts.

Sample	Cu content (%)
Fresh CuO/c-UiO-66	39.9
Spent CuO/c-UiO-66	24.8

Thermogravimetric analysis (TGA) revealed a small loss in weight of UiO-66 and CuO/c-UiO-66 starting below about 100 °C, which was attributed to the moisture contained in the material. As the temperature increases, the UiO-66 framework started to disintegrate, whereas CuO/c-UiO-66 was stable in the temperature range of 200 ~ 800 °C, indicating that the presence of CuO/c-UiO-66 was more stable at high temperatures (Fig. S1). This suggested that the addition of CuO might have a supporting effect on the UiO-66 derived framework.

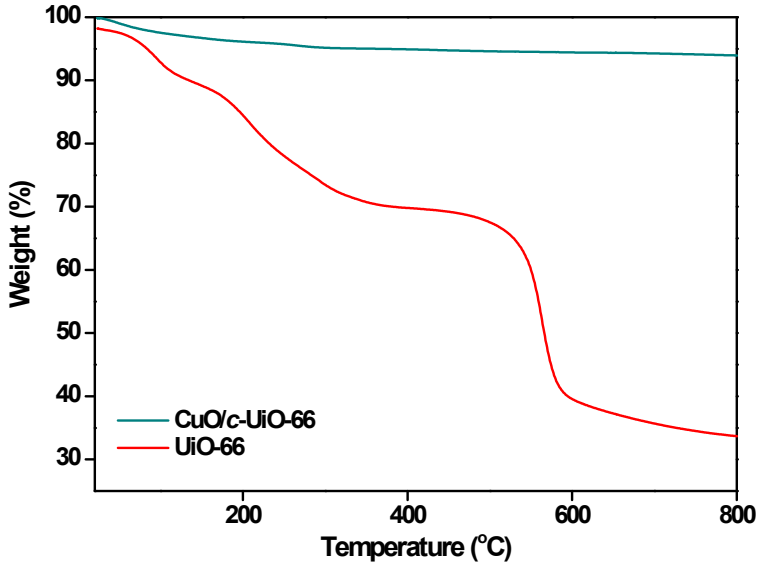

Fig. S1. Thermogravimetric analysis of UiO-66 and CuO/c-UiO-66.

Table S2. N_2 adsorption-desorption of UiO-66 and CuO/c-UiO-66 catalyst.

Sample	Specific surface area (m^2 g^{-1})[a]
UiO-66	294.7
CuO/c-UiO-66	69.1

[a] BET surface area.

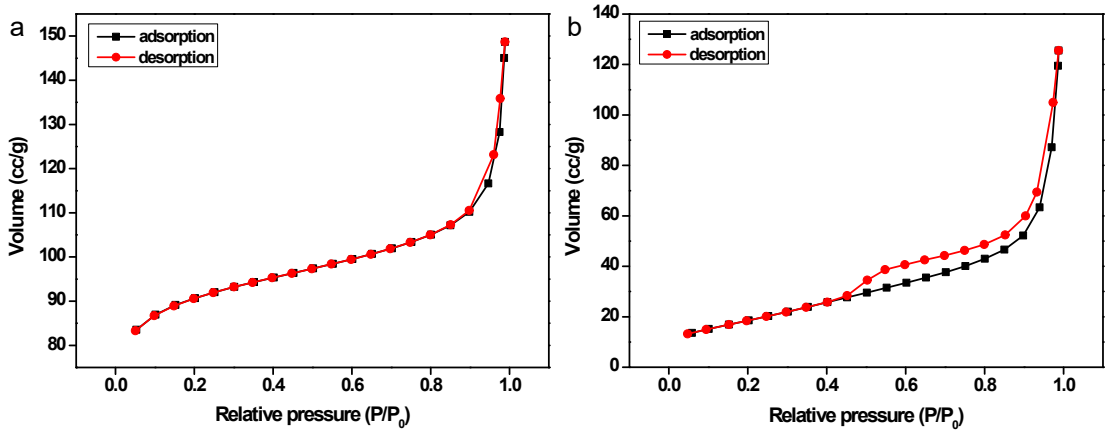

Fig. S2. N_2 adsorption-desorption isotherms of (a) UiO-66 and (b) CuO/c-UiO-66 catalyst.

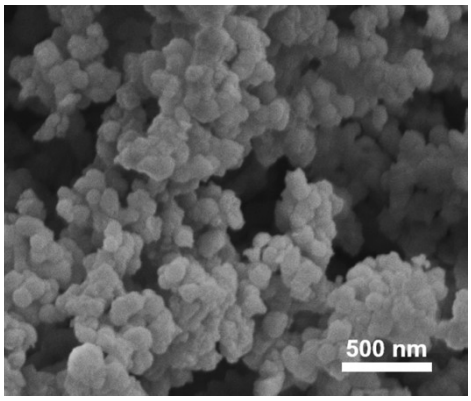

Fig. S3. SEM of CuO/c-UiO-66.

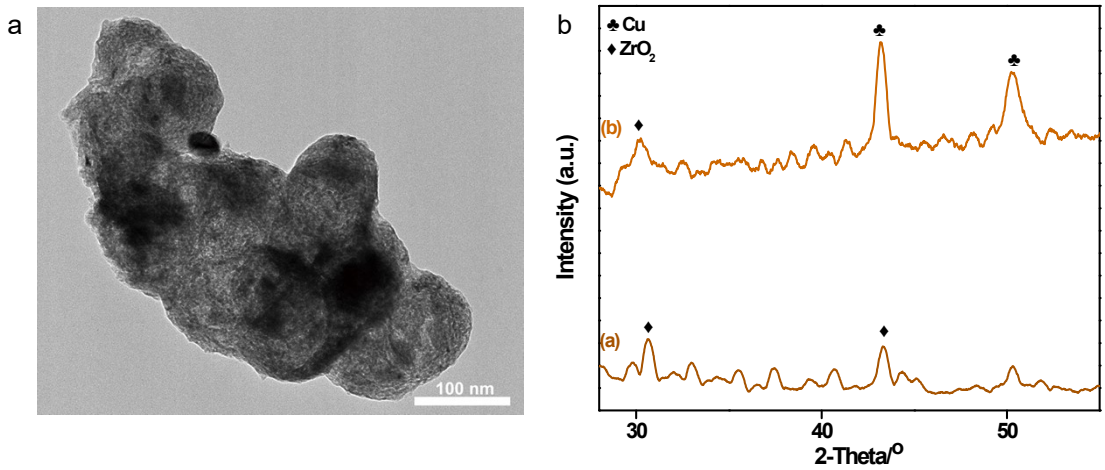

Fig. S4. (a) HADDF of spent CuO/c-UiO-66;(b) Powder XRD patterns of (a) UiO-66; (b) spent CuO/c-UiO-66.

The XRD pattern of the spent catalyst reflected the decrement of intensity of both ZrO_2 and CuO diffraction peaks, which might be due to the accumulation of small amounts of carbohydrate residues on the Cu/Zr oxide surface.

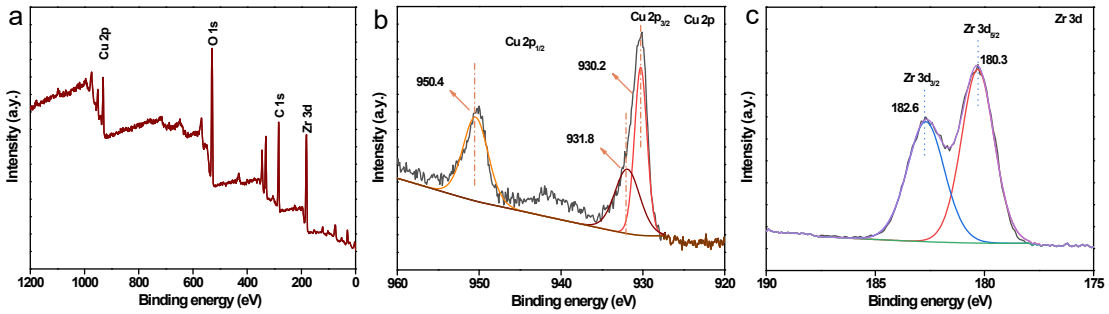

Fig. S5. XPS spectra of (a) all, (b) Cu 2p and (c) Zr 3d of spent CuO/c-UiO-66.

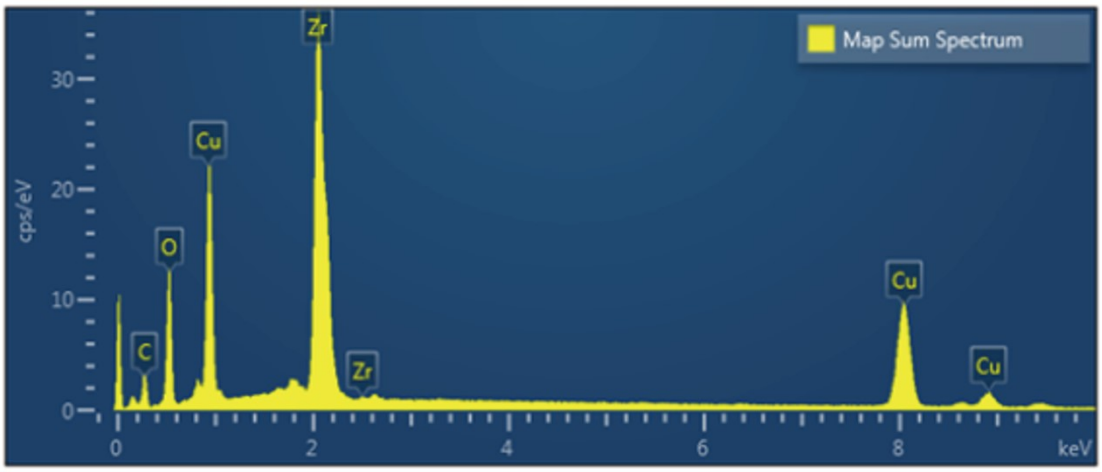

Fig. S6. SEM-EDS image of fresh CuO/c-UiO-66.

Table S3. Element content of fresh CuO/c-UiO-66.

Element	Apparent concentration	k ratio	wt%	Atomic (%)	Standard label
C	2.79	0.02794	14.94	36.95	C Vit
O	15.90	0.05350	20.42	37.91	SiO_2
Cu	38.32	0.38324	28.83	13.48	Cu
Zr	39.21	0.39213	35.82	11.67	Zr
Total			100.00	100.00	

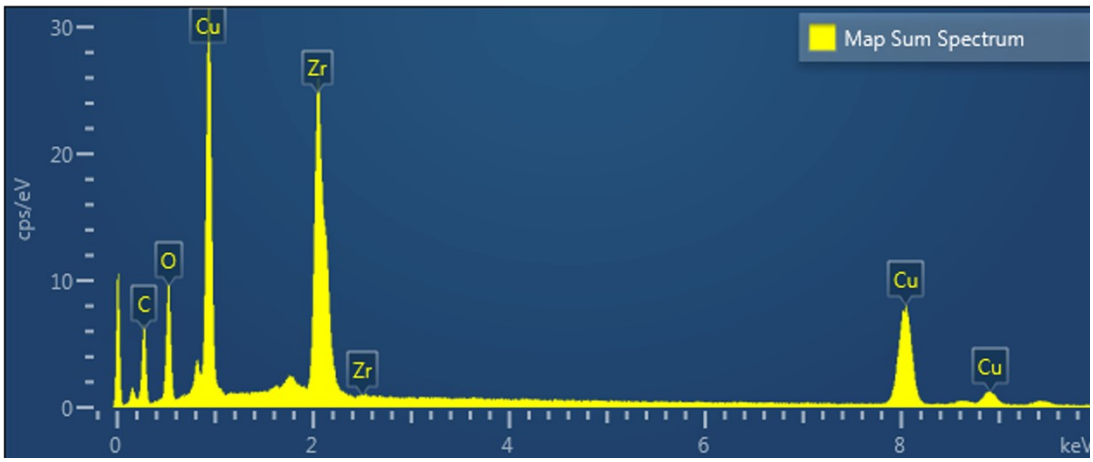

Fig. S7. SEM-EDS image of spent CuO/c-UiO-66.

Table S4. Element content of spent CuO/c-UiO-66.

Element	Apparent concentration	k atio	wt%	Atomic (%)	Standard label
C	6.41	0.06413	27.86	55.77	C Vit
O	13.95	0.04693	17.81	26.76	SiO_2
Cu	37.40	0.37401	27.42	10.38	Cu
Zr	31.31	0.31306	26.91	7.09	Zr
Total			100.00	100.00	

4. Chemical composition of sawdust

Firstly, the sawdust (particles size: 0.5 ~ 1.0 mm) was extracted with toluene/ethanol (2:1, v/v) in a Soxhlet instrument for 12 h, and then dried at 50 °C under vacuum for 8 h. The chemical compositions of variously woody sawdust were analyzed according to the National Renewable Energy Laboratory (NREL) standard analytical procedure with a minor modification.[7] Typically, woody sawdust (300 mg) was hydrolyzed with 72 wt% sulfuric acid solution (3.0 mL) at 30 °C for 1 h. Deionized water (84.0 mL) was then added to dilute sulfuric acid (ca. 3%). This mixture was heated at 120 °C for 1 h in an autoclave. After cooling, the mixture was filtered through a mixed cellulose ester (MCE) membrane filter (0.2 μm). The amount of acid insoluble lignin (AIL, Klason lignin) was determined by measurement the weight of residue after drying. The concentration of acid soluble lignin (ASL) was determined by UV spectra by measuring the absorbance of the soluble fraction at 205 nm. The concentrations of the monosaccharides were determined by high performance anion exchange chromatography with pulsed amperometry detection (HPAEC-PAD).

Table S5. The composition of hardwood sawdust.[a]

Entry	Substrate	AIL (wt%)[b]	ASL (wt%)[c]	Cellulose (wt%)	Hemicellulose (wt%)
1	Poplar	22.4	2.5	42.7	19.7
2	Eucalyptus	26.6	1.9	40.3	22.7
3	Beech	20.3	2.8	42.1	26.8
4	Birch	27.3	1.7	44.2	26.4

[a] The compositions of biomass were analyzed according to the procedures of the NREL method.

[b] AIL: acid insoluble lignin (Klason lignin).

[c] ASL: acid soluble lignin.

Table S6. The sugar retention of poplar after the reductive catalytic deconstruction of lignin into phenolic monomers over a CuO/c-UiO-66 catalyst.[a]

Entry	Substrate	Temperature (°C)	Time (h)	Sugar retention (wt%)		
				C5	C6	Total[b]
1	Poplar	240	2	14.5	61.8	76.3

[a] Reaction condition: poplar sawdust (50 mg), CuO/c-UiO-66 (20 mg), MeOH (10 mL), H_2 (3 MPa).

[b] Based on the amount of C5, C6 in the sugar fractions of poplar sawdust.

5. Preparation for double enzymatic lignin (DEL)

Double enzymatic lignin (DEL), as a representative whole lignin sample of lignocellulosic biomass, could better delineate the structural characteristic of the lignin macromolecule.[8] Accordingly, the dewaxed wood samples were firstly ball-milled using a Fritsch Planetary Mill Pulverisette 5 (Germany) with zirconium dioxide (ZrO_2) vessels containing ZrO_2 ball bearings (10 mm × 10) under 400 rpm for 4 h. One cycle of the ball-milling condition consisted of a 5-min milling and a 5-min cooling cycle. Then, the ball-milled wood powder (5 g) was subjected to digestion in 100 mL acetate buffer (0.05 mM, pH 4.8) with loading of 2.5 mL of cellulase and 0.5 mL hemicellulose. The reaction mixture was incubated at 50 °C in a rotary shaker (150 rpm) for 48 h. Subsequently, the mixture was centrifuged, and the residual solid was extensively washed with acetate buffer (pH 4.8) and hot water and then freeze-dried. After that, the obtained solid further underwent the same enzymatic hydrolysis after the ball-milling (2 h) process. Finally, the DEL samples were achieved after centrifugation and lyophilization.

6. Catalytic hydrogenolysis of woody biomass

General procedure

In a typical rection, woody sawdust (50 mg), CuO/c-UiO-66 (20 mg) and MeOH (10 mL) were charged into a 50 mL Parr autoclave. The reactor was sealed, purged with nitrogen, and then was pressured to H_2 (3 MPa) at room temperature. The reaction was carried out at different temperatures for a certain time with a magnetic stirring at 800 rpm. After completion, the autoclave was cooled (2.8 ~2.9 MPa) and depressurized carefully. Then the reaction mixture was filtered, and the insoluble fraction was washed with dichloromethane. Subsequently, the solution fraction was extracted with dichloromethane (DCM) and the resulting lignin oily product was obtained after removing all volatiles under vacuum condition. An external standard (1,3,5-trimethoxybenzene) was added to the lignin oil solution in dichloromethane, which was subjected to GC and GC-MS for analysis. The identification and quantification of lignin monomers in the oily product were assessed by comparison with authentic samples acquired from commercial purchase or independent synthesis. In the case of commercial catalysts, 20 mg Ru/C (Ru content: 5 wt%) or 20 mg Pd/C (Pd content: 5 wt%) were used for the hydrogenolysis of poplar sawdust (50 mg).

7. Lignin products analysis

Monomers analysis

Gas chromatography (GC) and Gas chromatography-mass spectrometry (GC-MS) analyses were performed on a Shimadzu Model 2010 plus with a HP-5 column (30 m × 0.25 mm × 0.25 mm) employing a flame ionization detector (FID) and a Shimadzu GCMS-QP2010SE with a HP-5MS (30 m × 0.25 mm × 0.25 mm) column, respectively. Injecting temperature was 250 °C. A column temperature procedure of 50 °C in 3 min, and 8 °C min^{-1} to 280 °C. The injection temperature of FID was 200 °C. The characterization and quantification lignin monomers within oil-based products has been estimated by reference to real samples obtained from commercial source or independent synthesis. The monomer yields were calculated using the formula:

$$\text{Monomer yield (wt\%)} = \frac{Mass\ (monomer)}{Mass\ (initial\ lignin)} \times 100\ \% \quad (1)$$

$$\text{Monomer yield (\%)} = \frac{Mole\ (monomer)}{Mole\ (lignin\ mimics)} \times 100\ \% \quad (2)$$

Delignification

For the soluble fraction, the dichloromethane was removed under vacuum to give crude "lignin oil", which was weighted to determine the degree of delignification (based on Klason lignin weight).

$$\text{Delignification (wt\%)} = \frac{Mass(lignin\ oil)}{Mass\ (initial\ lignin)} \times 100\ \%$$

Gel permeation chromatography (GPC) analysis

Gel permeation chromatography (GPC) analysis were conducted on an Agilent Plgel 3 μm 100 Å 300 × 7.5 mm column equipped with an automatic injector (Waters 717), and a Double Absorbance UV detector (Waters 2487), and calibrated using polystyrene standards (peaks average molecular weights of 96500, 1320, 9200, 66000, Ploymer Laboratories Ltd.).

GPC investigated the molar mass distribution of both lignin and oil after RCD.

Lignin from different woods were analyzed after acetylation as shown below: raw lignin product (100 mg) was prepared by treatment with 1:1 acetic anhydride and pyridine mix solution (2.5 mL) in room temperature for 48 h. The acetylated products were put in cold deionized water immediately and rinsed with deionized water. The acetylated product was dissolved after vacuum evaporation to THF (2 mg mL^{-1}) and purified through a 0.45 μm syringe filter at the time of injection.[9]

GPC analysis of lignin oil (THF solution, ~2 mg mL^{-1}) was performed on an Agilent 1260 with seven GPC polystyrene standards (124 ~ 26520 g mol^{-1}) for calibration.

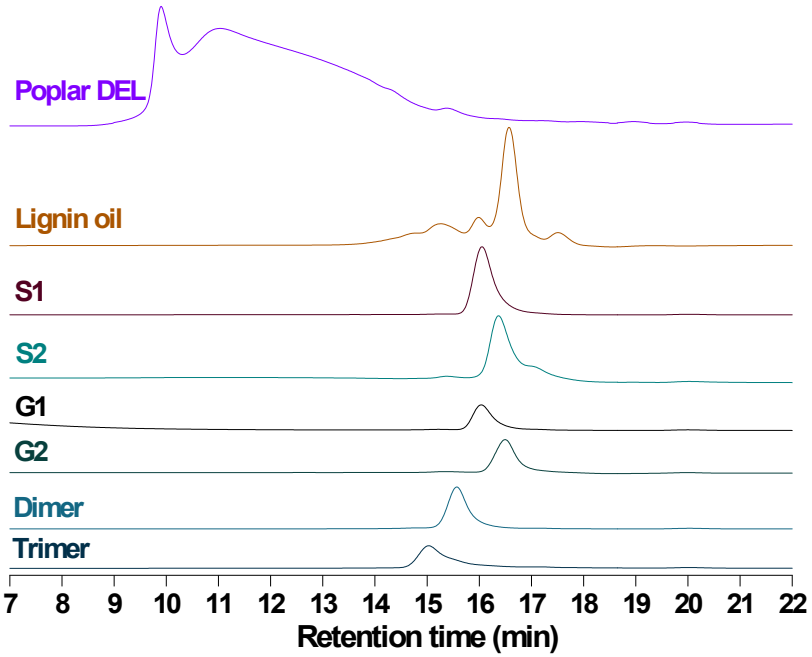

Fig. S8. GPC of lignin monomer, dimer, trimer, and lignin oily product from catalytic hydrogenolysis of poplar sawdust over a CuO/c-UiO-66 catalyst.

Table S7. Catalyzed hydrogenolysis of poplar sawdust with d-UiO-66, ZrO_2, CuO and with or without catalyst.[a]

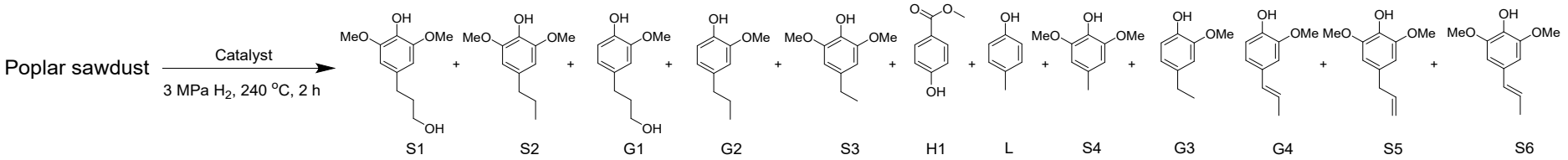

Entry	Catalyst	S1	S2	Monomer yield (wt%)										Total yield (wt%)	Delignification (wt%)[c]
				G1	G2	S3	H1	L	S4	G3	G4	S5	S6		
1	d-UiO-66	ND[b]	ND	ND	ND	ND	5.1	ND	ND	ND	ND	ND	3.3	8.4	45
2	No	ND	ND	ND	ND	ND	4.6	ND	ND	ND	ND	ND	2.1	6.7	40
3	ZrO_2	ND	ND	ND	ND	ND	3.2	ND	ND	ND	ND	ND	6.8	10.0	52
4	CuO	7.8	1.1	4.5	0.6	ND	1.4	ND	ND	ND	1.0	4.2	2.0	22.6	78
5	CuO/c-UiO-66	14.7	9.9	5.6	3.0	3.3	2.9	1.4	1.0	1.0	ND	ND	ND	42.8	91

[a] Reaction conditions: Poplar sawdust (50 mg), catalyst (20 mg), MeOH (10 mL), H_2 (3 MPa), 240 ℃, 2 h.

[b] ND, not detectable.

[c] Based on the weight of dichloromethane extracted fraction (Klason lignin).

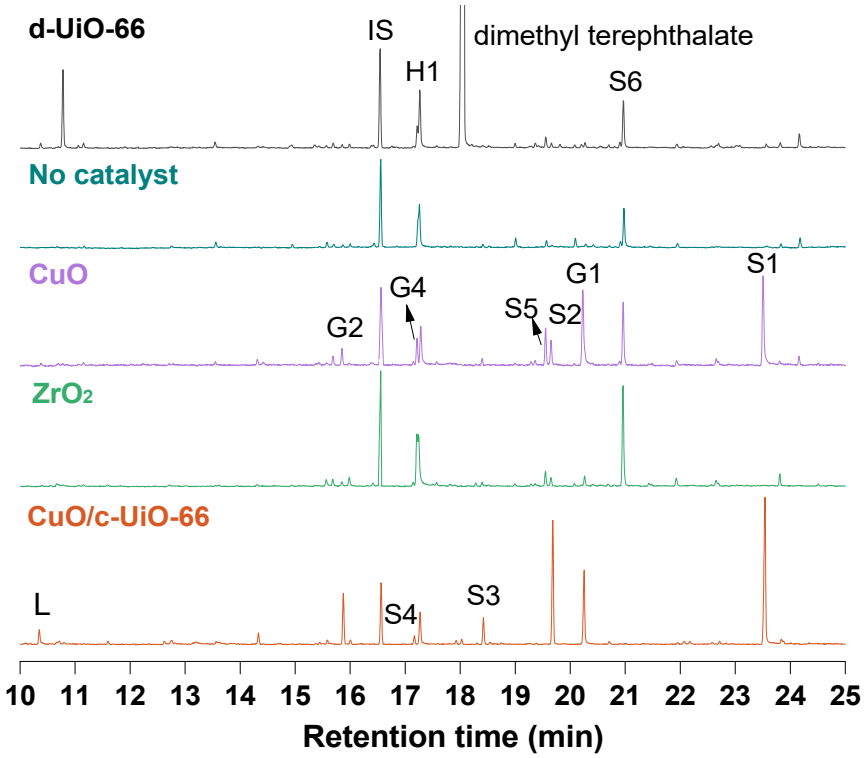

Fig. S9. Gas chromatogram of the monomers from reductive catalytic deconstruction of lignin from poplar sawdust with different catalysts.

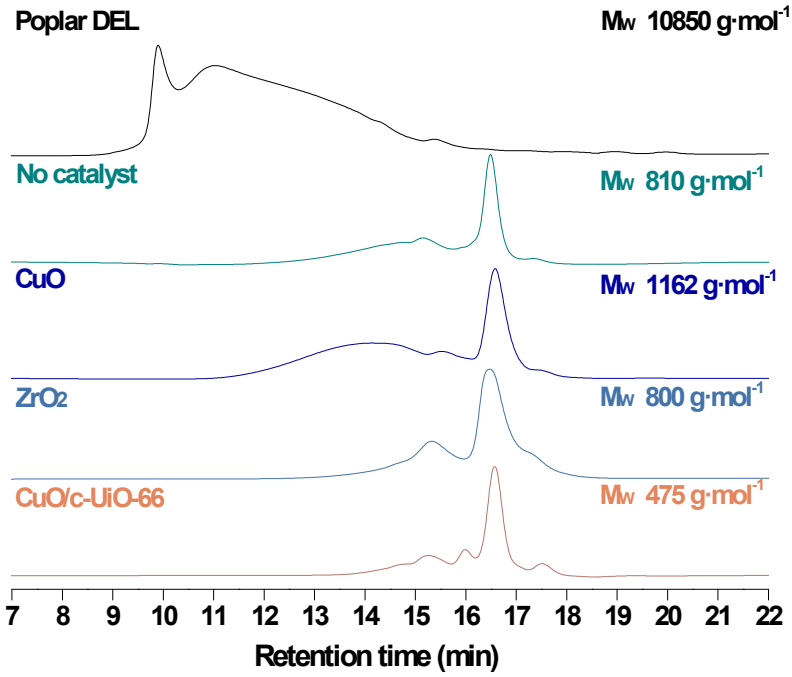

Fig. S10. GPC of lignin oil products from reductive catalytic deconstruction of lignin from poplar sawdust with different catalysts.

Table S8. Catalyzed hydrogenolysis of poplar sawdust with CuO/c-UiO-66 under different molar ratios of Cu/Zr.[a]

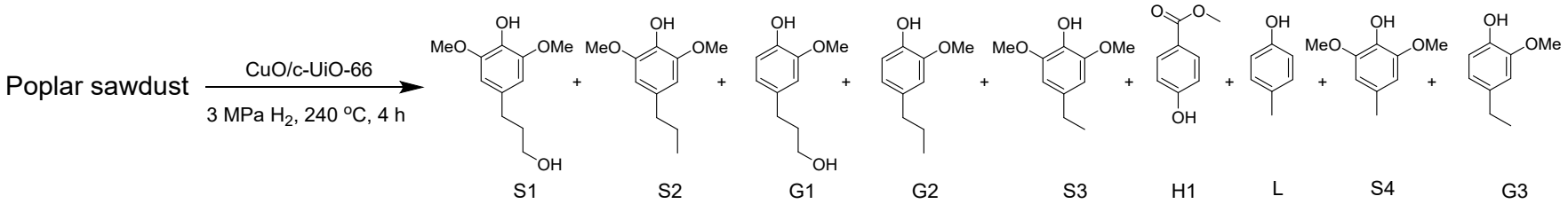

Entry	Cu/Zr	Monomer yield (wt%)									Total yield (wt%)	Delignification (wt%)
		S1	S2	G1	G2	S3	H1	L	S4	G3		
1	0.8	13.4	8.9	5.4	3.0	3.0	2.7	1.5	1.0	1.0	39.9	88
2	1.2	15.0	10.0	5.7	3.1	2.9	2.3	1.8	1.1	1.0	42.9	91
3	1.6	14.8	9.7	5.8	3.1	3.1	2.7	1.5	1.4	0.9	43.0	91
4	2.0	12.2	7.6	5.4	2.4	2.2	2.8	0.9	0.9	0.7	35.1	85

[a] Reaction conditions: Poplar sawdust (50 mg), MeOH (10 mL), H_2 (3 MPa), 240 °C, 4 h.

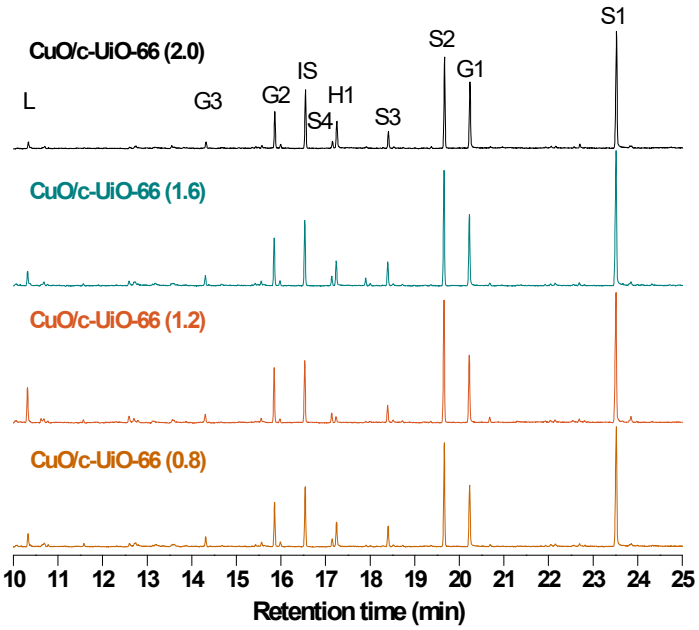

Fig. S11. Gas chromatogram of the monomers from reductive catalytic deconstruction of lignin from poplar over a CuO/c-UiO-66 catalyst with different molar ratios of Cu/Zr.

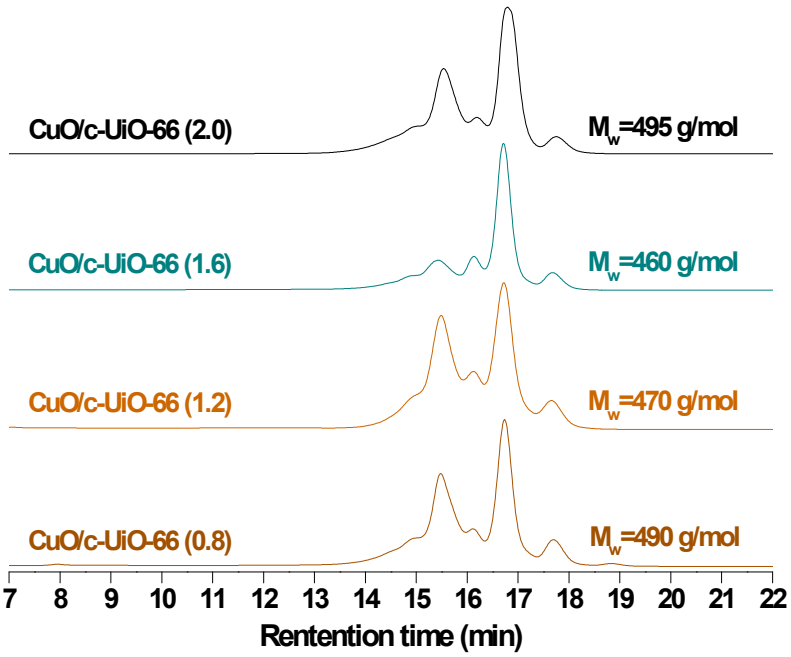

Fig. S12. GPC of lignin oil products from reductive catalytic deconstruction of lignin from poplar sawdust with different molar ratios of Cu/Zr.

Table S9. Catalyzed hydrogenolysis of poplar sawdust with different catalysts.[a]

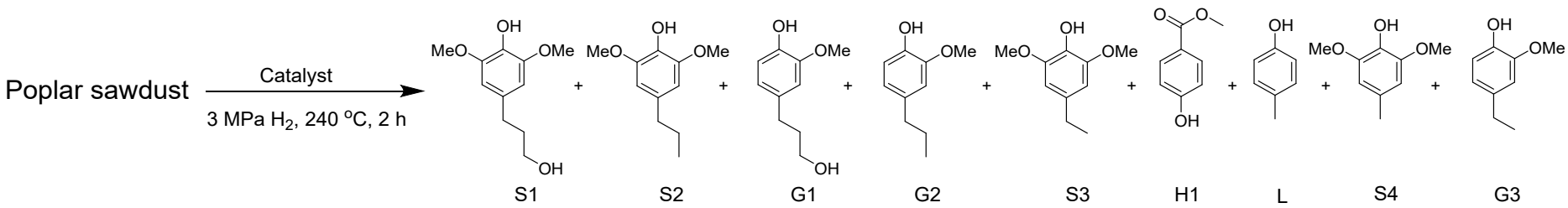

Entry	Catalyst	Monomers yield (wt%)									Total yield (wt%)	Delignification (wt%)
		S1	S2	G1	G2	S3	H1	L	S4	G3		
1	Pd/C	15.5	3.9	8.1	0.5	5.1	2.2	ND	0.5	1.1	36.9	88
2	Ru/C	2.7	20.9	1.3	7.1	1.2	2.2	ND	ND	ND	35.4	86
3	CuO/c-UiO-66	14.7	9.9	5.6	3.0	3.3	2.9	1.4	1.0	1.0	42.8	91

[a] Reaction conditions: Poplar sawdust (50 mg), MeOH (10 mL), H_2 (3 MPa), 240 °C, 2 h.

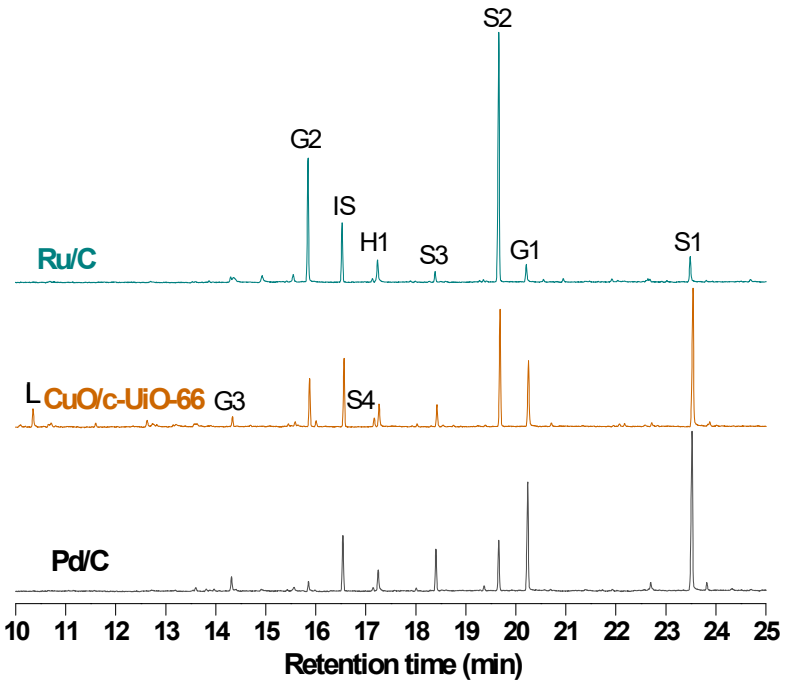

Fig. S13. Gas chromatogram of the monomers from reductive catalytic deconstruction of lignin from poplar sawdust with different catalysts.

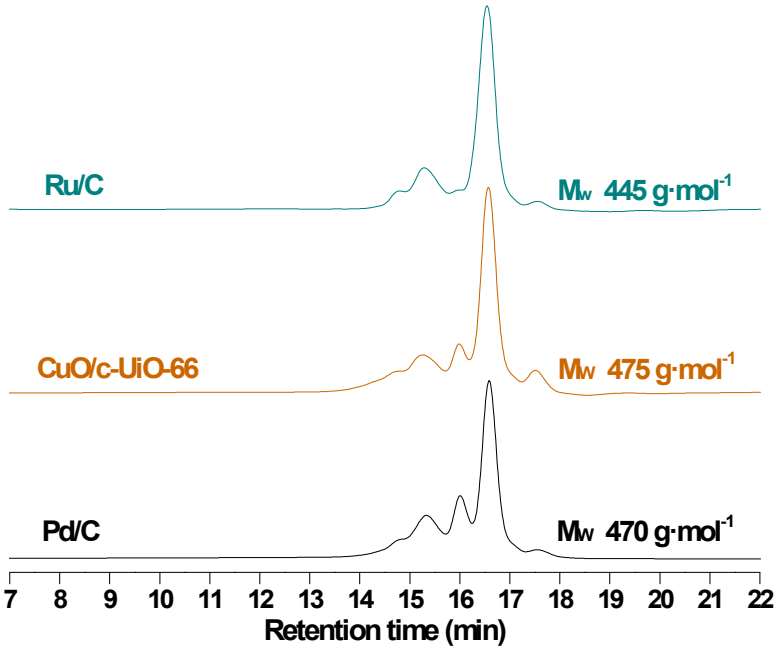

Fig. S14. GPC of lignin oil products from reductive catalytic deconstruction of lignin from poplar sawdust with different catalysts.

Table S10. Catalyzed hydrogenolysis of poplar sawdust with CuO/c-UiO-66 with different catalyst dosages.[a]

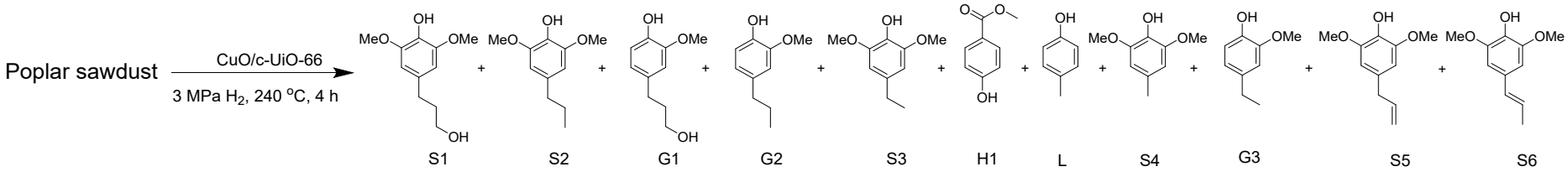

Entry	Catalyst dosage (mg)	Monomer yield (wt%)											Total yield (wt%)	Delignification (wt%)
		S1	S2	G1	G2	S3	H1	L	S4	G3	S5	S6		
1	10	13.2	6.6	5.7	2.2	1.7	3.7	ND	0.9	0.8	0.5	1.0	36.3	83
2	15	14.0	9.0	5.1	2.9	3.3	2.7	1.2	0.9	1.0	ND	ND	40.1	86
3	20	15.0	10.0	5.7	3.1	2.9	2.3	1.8	1.1	1.0	ND	ND	42.9	91
4	25	11.5	8.6	4.1	2.6	2.7	1.4	1.6	1.1	0.90	ND	ND	34.5	80

[a] Reaction conditions: Poplar sawdust (50 mg), MeOH (10 mL), H_2 (3 MPa), 240 °C, 4 h.

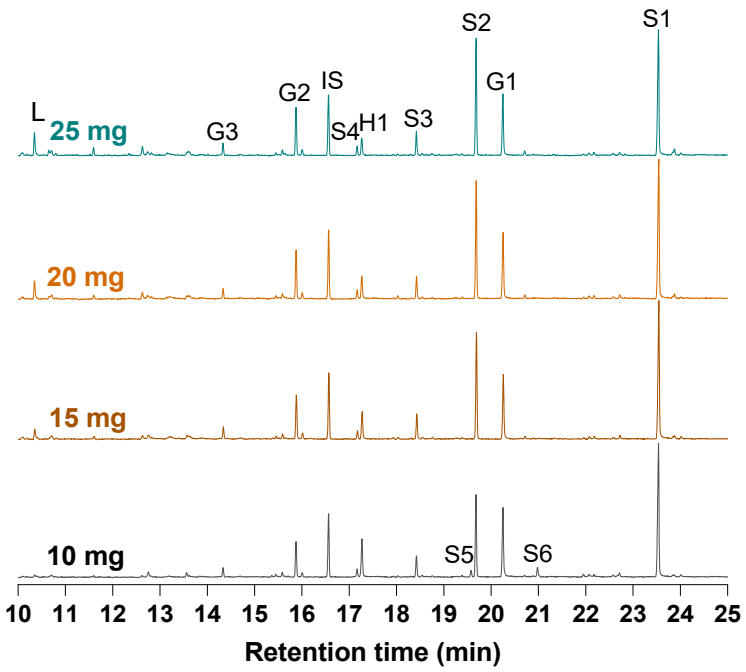

Fig. S15. Gas chromatogram of the monomers from reductive catalytic deconstruction of lignin from poplar sawdust with different catalyst dosages.

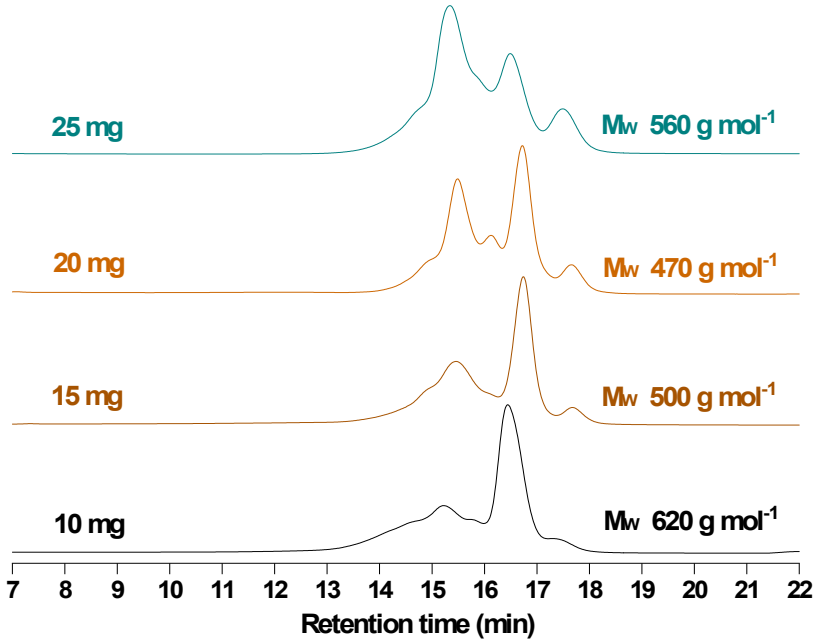

Fig. S16. GPC of lignin oil products from reductive catalytic deconstruction of lignin from poplar sawdust with different catalyst dosages.

Table S11. Catalyzed hydrogenolysis of poplar sawdust with CuO/c-UiO-66 with different solvents.[a]

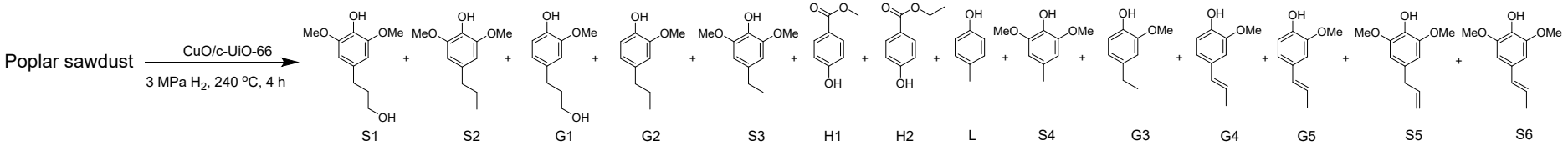

Entry	Solvent	Monomer yield (wt%)														Total yield (wt%)	Delignification (wt%)
		S1	S2	G1	G2	S3	H1	H2	L	S4	G3	G4	G5	S5	S6		
1	MeOH	15.0	10.0	5.7	3.1	2.9	2.3	ND	1.8	1.1	1.0	ND	ND	ND	ND	42.9	91
2	EtOH	12.1	4.6	12.0	1.8	0.4	ND	0.7	0.6	0.5	0.6	0.9	ND	ND	1.1	35.3	79
3	^{i}PrOH	2.6	1.1	1.3	0.3	0.5	ND	ND	ND	ND	ND	5.9	1.4	1.9	5.8	20.8	73
4	Dioxane	10.4	2.7	5.1	1.0	1.2	ND	ND	1.1	0.4	0.5	0.5	ND	0.3	1.8	25.0	78

[a] Reaction conditions: Poplar sawdust (50 mg), MeOH (10 mL), H_2 (3 MPa), 240 °C, 4 h.

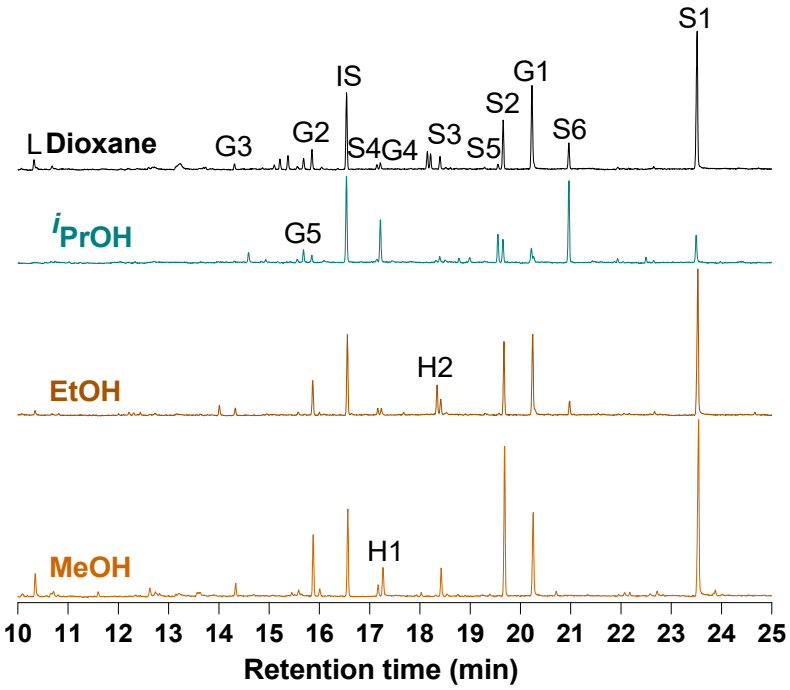

Fig. S17. Gas chromatogram of the monomers from reductive catalytic deconstruction of lignin from poplar sawdust over a CuO/c-UiO-66 catalyst with different solvents.

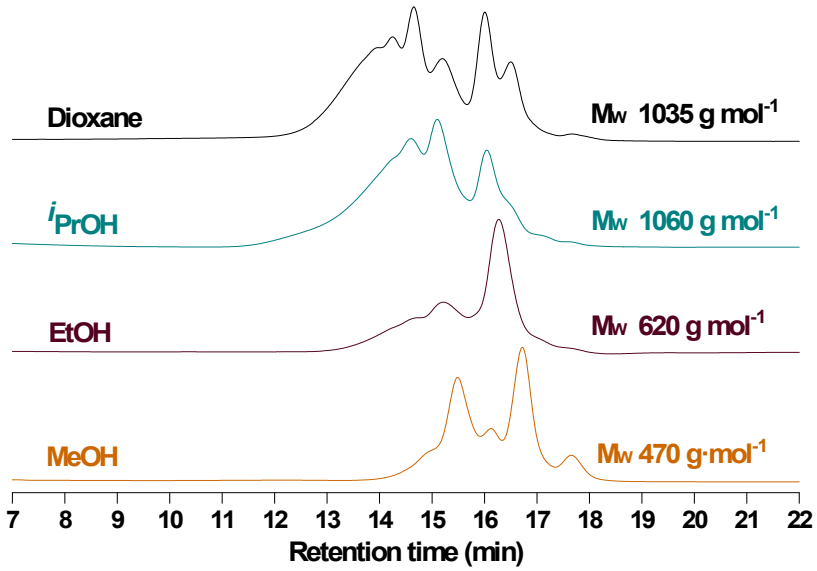

Fig. S18. GPC of lignin oil products from reductive catalytic deconstruction of lignin from poplar over a CuO/c-UiO-66 catalyst with different solvents.

Table S12. Catalyzed hydrogenolysis of poplar sawdust with CuO/c-UiO-66 with different temperatures.[a]

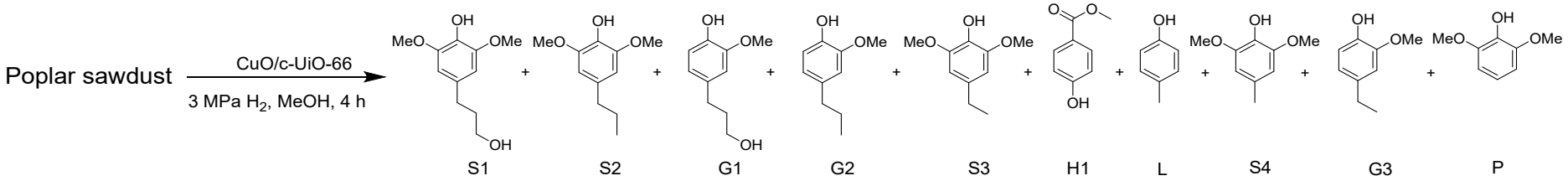

Entry	Temperature (°C)	Monomer yield (wt%)											Total yield (wt%)	Delignification (wt%)
		S1	S2	G1	G2	S3	H1	H2	L	S4	G3	P		
1	200	15.0	10.0	5.7	3.1	2.9	2.3	ND	1.8	1.1	1.0	ND	42.9	91
2	220	12.1	4.6	12.0	1.8	0.4	ND	0.7	0.6	0.5	0.6	ND	35.3	79
3	240	2.6	1.1	1.3	0.3	0.5	ND	ND	ND	ND	ND	ND	20.8	73
4	260	10.4	2.7	5.1	1.0	1.2	ND	ND	1.1	0.4	0.5	0.8	25.0	78

[a] Reaction conditions: Poplar sawdust (50 mg), CuO/c-UiO-66 (20 mg), MeOH (10 mL), H_2 (3 MPa), 4 h.

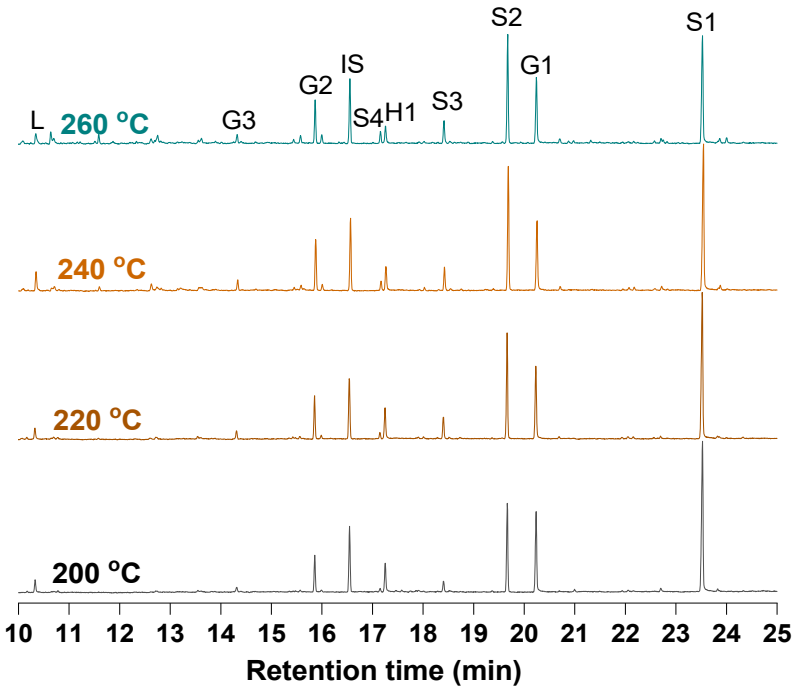

Fig. S19. Gas chromatogram of the monomers from reductive catalytic deconstruction of lignin from poplar over a CuO/c-UiO-66 catalyst with different temperatures.

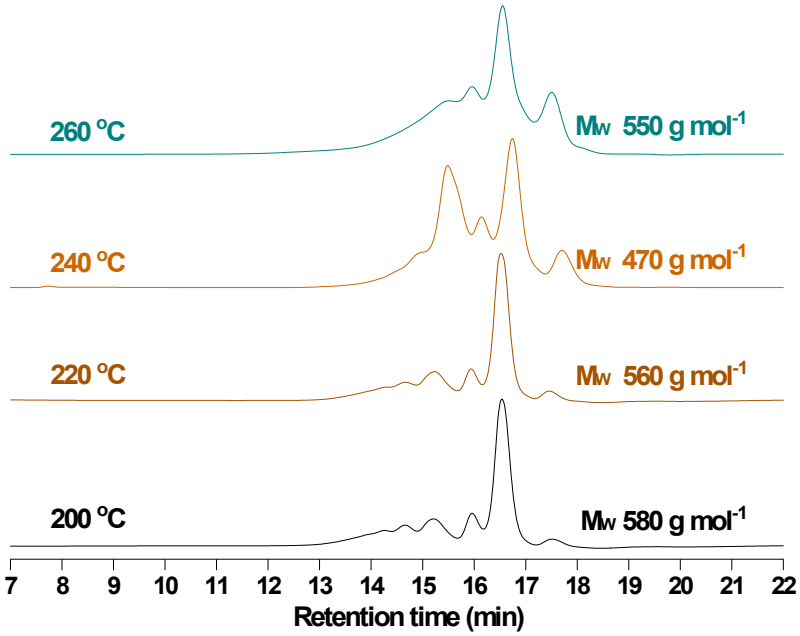

Fig. S20. GPC of lignin oil products from reductive catalytic deconstruction of lignin from poplar sawdust over a CuO/c-UiO-66 catalyst with different temperatures.

Table S13. Catalyzed hydrogenolysis of poplar sawdust with CuO/c-UiO-66 with different times.[a]

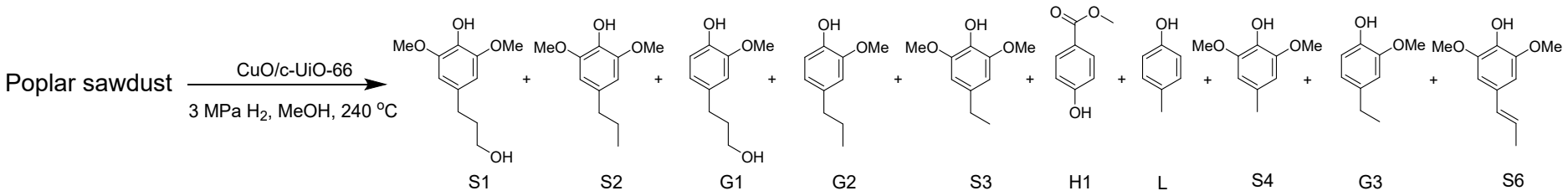

Entry	Time (h)	Monomers yield (wt%)										Total yield (wt%)	Delignification (wt%)
		S1	S2	G1	G2	S3	H1	L	S4	G3	S6		
1	0.5	11.5	3.9	5.0	1.4	1.5	3.1	ND	0.5	0.5	1.4	28.8	74
2	1	13.7	7.7	5.6	2.5	2.2	3.1	0.9	0.7	0.7	ND	37.2	82
3	2	14.7	9.9	5.6	3.0	3.3	2.9	1.4	1.0	1.0	ND	42.8	91
4	4	15.0	10.0	5.7	3.1	2.9	2.3	1.8	1.1	1.0	ND	42.9	91
5	6	14.4	10.0	5.2	3.0	3.5	1.6	1.9	1.2	1.0	ND	41.8	90

[a] Reaction conditions: Poplar sawdust (50 mg), CuO/c-UiO-66 (20 mg), MeOH (10 mL), H_2 (3 MPa).

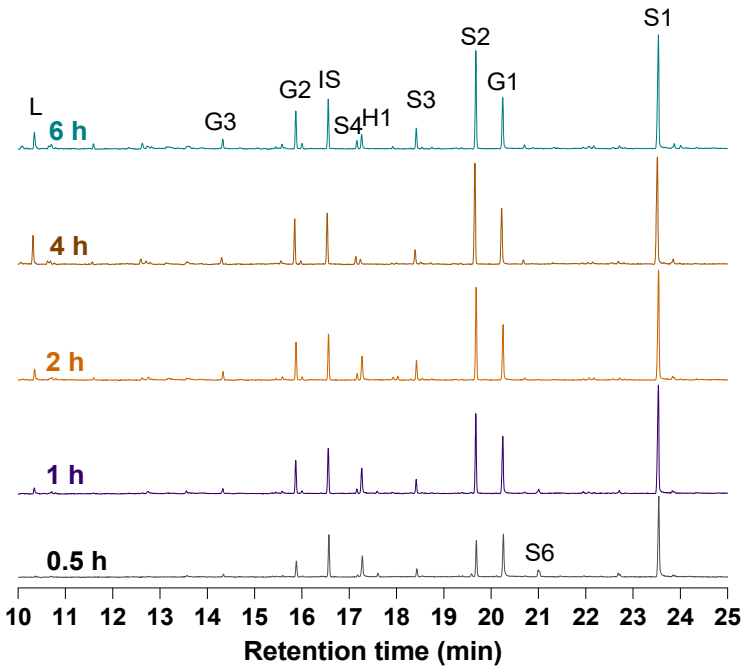

Fig. S21. Gas chromatogram of the monomers from reductive catalytic deconstruction of lignin from poplar sawdust over a CuO/c-UiO-66 catalyst with different reaction times.

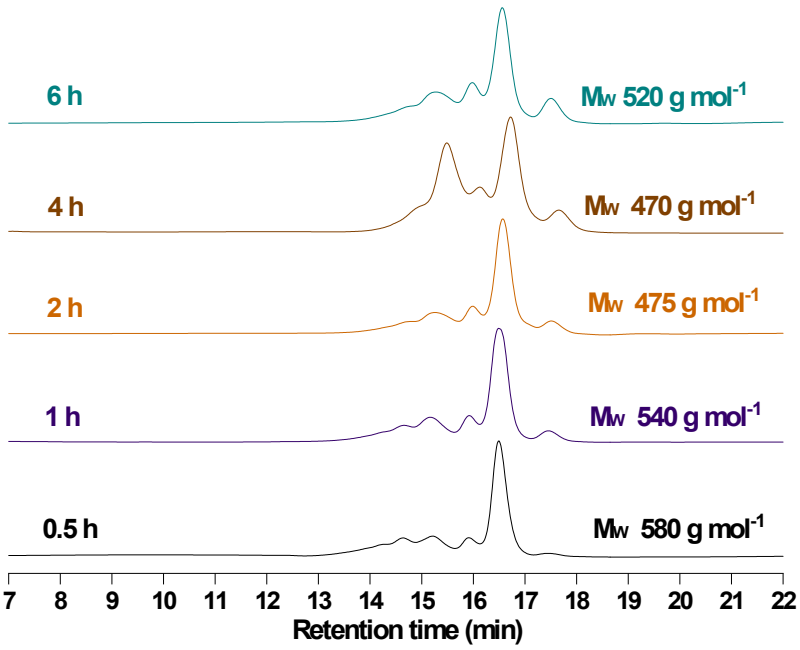

Fig. S22. GPC of lignin oil products from reductive catalytic deconstruction of lignin from poplar sawdust over a CuO/c-UiO-66 catalyst with reaction times.

Table S14. Catalyzed hydrogenolysis of poplar sawdust with CuO/c-UiO-66 with different recycle times.

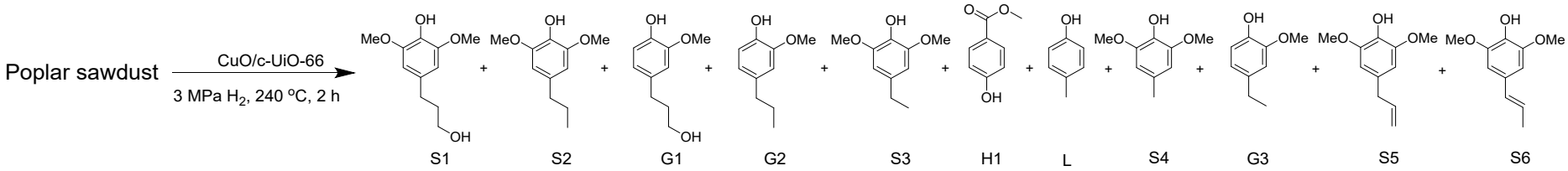

Entry	Run	Monomers yield (wt%)											Total yield (wt%)	Delignification (wt%)
		S1	S2	G1	G2	S3	H1	L	S4	G3	S5	S6		
1[a]	1	14.7	9.9	5.6	3.0	3.3	2.9	1.4	1.0	1.0	ND	ND	42.8	91
2[b]	2	7.1	2.7	1.4	4.4	0.9	3.3	ND	0.3	0.6	2.7	3.3	26.7	85
3[c]	3	3.6	0.7	0.5	2.4	1.0	3.2	ND	ND	0.4	3.1	0.8	15.7	66

[a] Reaction conditions: Poplar sawdust (100 mg), CuO/c-UiO-66 (40 mg), MeOH (20 mL), H_2 (3 MPa),240 °C, 2 h.

[b] Fresh CuO/c-UiO-66 was used.

[c] Spent CuO/c-UiO-66 was used.

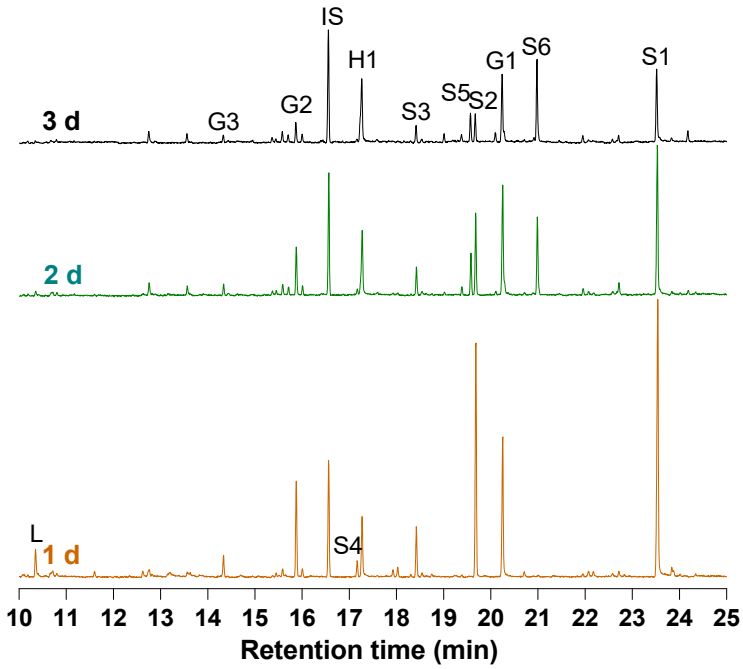

Fig. S23. Gas chromatogram of the monomers from reductive catalytic deconstruction of lignin from poplar sawdust over a CuO/c-UiO-66 catalyst with different recycle times.

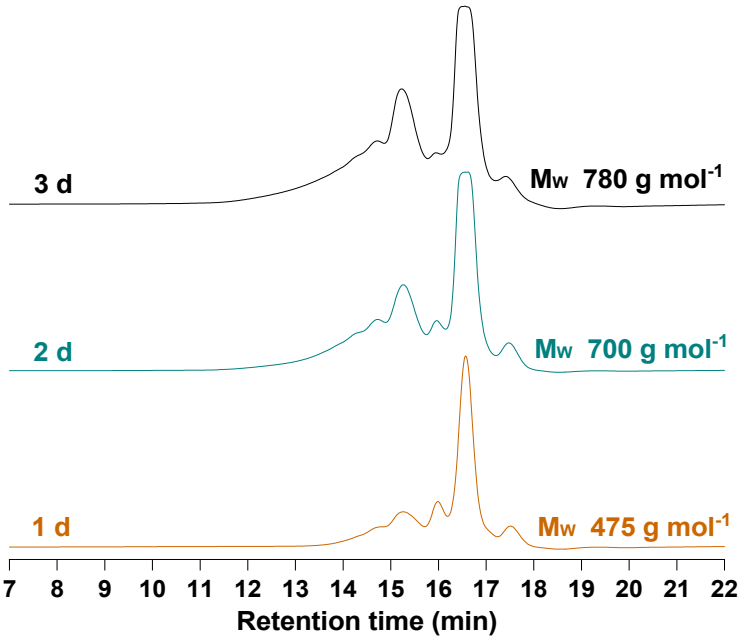

Fig. S24. GPC of lignin oil products from reductive catalytic deconstruction of lignin from poplar over a CuO/c-UiO-66 catalyst with different recycle times.

Table S15. Catalyzed hydrogenolysis of different wood sawdust with CuO/c-UiO-66.[a]

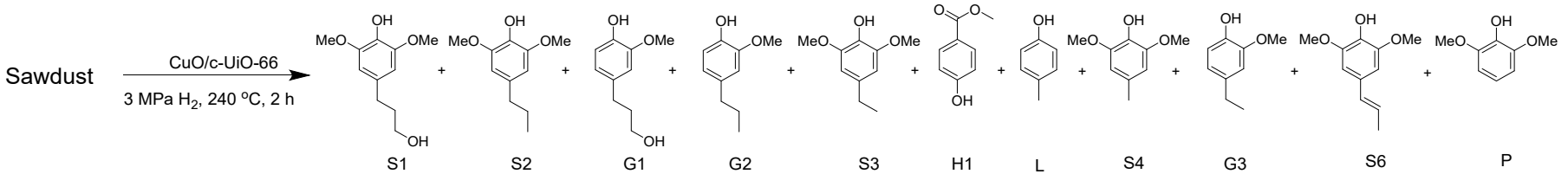

Entry	Sawdust	Monomers yield (wt%)											Total yield (wt%)	Delignification (wt%)
		S1	S2	G1	G2	S3	H1	L	S4	G3	S6	P		
1	Poplar	14.7	10.0	5.6	3.0	3.3	2.9	1.4	1.0	1.0	ND	ND	42.8	91
2	Eucalyptus	13.7	8.3	6.2	2.3	2.5	ND	ND	0.7	0.7	ND	ND	34.4	88
3	Beech	14.2	9.9	4.4	1.9	3.2	ND	ND	1.1	0.7	1.0	0.8	37.2	85
4	Birch	8.7	6.3	2.8	1.3	2.1	ND	ND	0.6	0.6	ND	0.5	22.9	82

[a] Reaction conditions: Poplar sawdust (50 mg), CuO/c-UiO-66 (20 mg), MeOH (10 mL), H_2 (3 MPa),240 °C, 2 h.

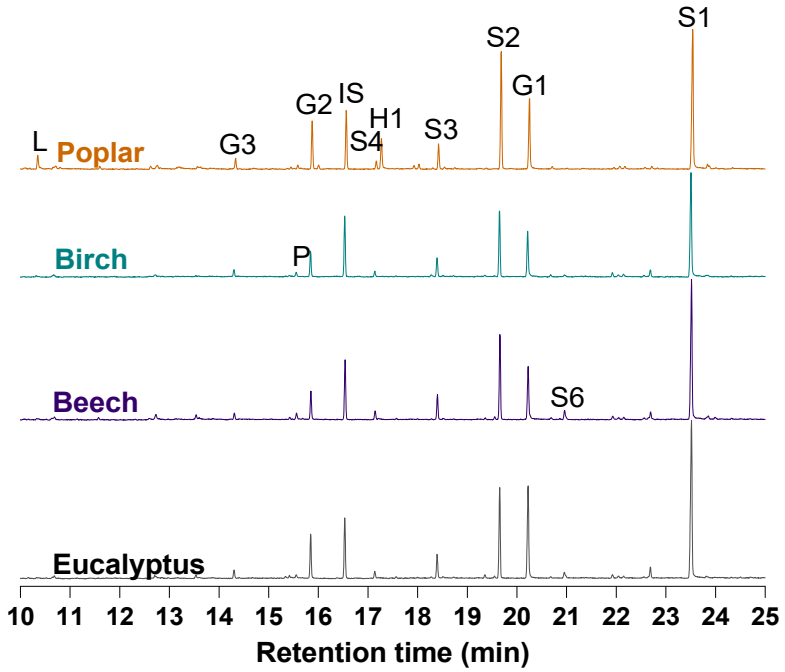

Fig. S25. Gas chromatogram of the monomers from reductive catalytic deconstruction of lignin from different sawdust over a CuO/c-UiO-66 catalyst.

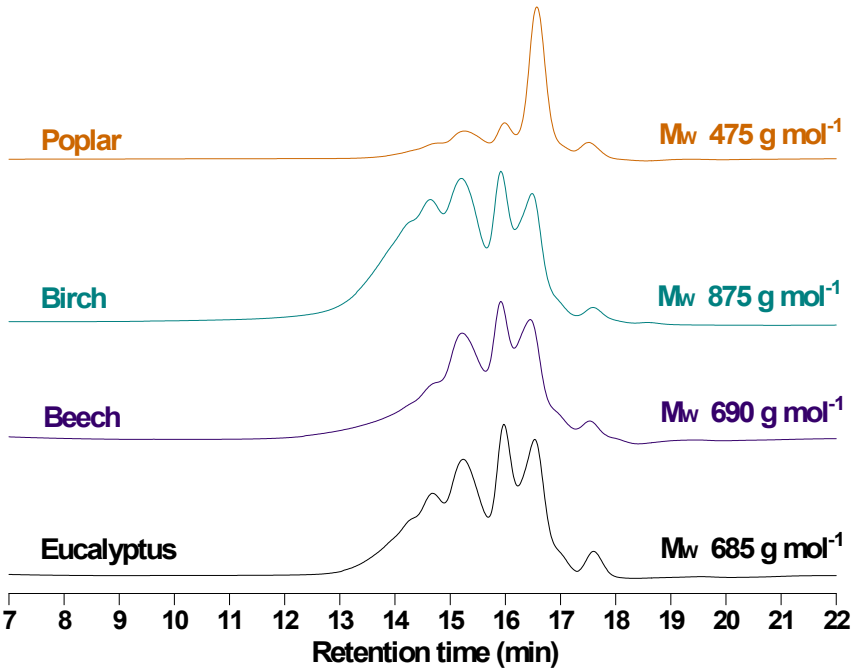

Fig. S26. GPC of lignin oil products from reductive catalytic deconstruction of lignin from different sawdust over a CuO/c-UiO-66 catalyst.

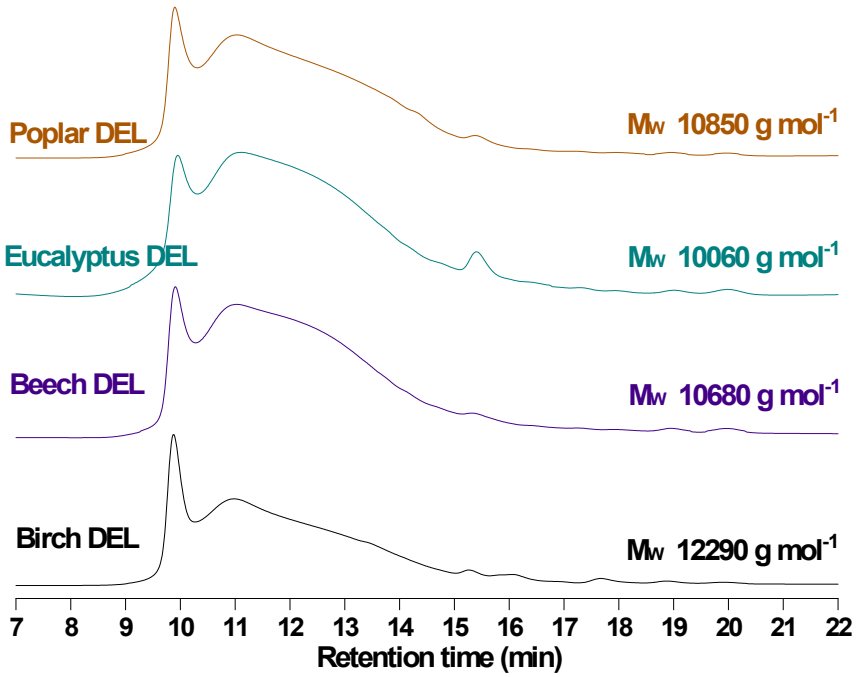

Fig. S27. GPC of DELs isolated from different hardwoods.

Table S16. The hydrogenolysis activity of lignocellulose with the state-of-the-art catalyst.[a]

Substrate	Catalyst	Reaction condition			Yield (wt%)	Reference
		Solvent	Temperature (°C)	Time (h)		
Birch	Ni-Al_2O_3	MeOH	250	3	44	10
Pine	Cu20-PMO	MeOH	220	18	36	11
Eucalyptus	MoO_x/SBA-15	MeOH	260	4	43.4	12
Birch	Co-phen/C	EtOH/H_2O (1:1 v/v), HCOOH, HCOONa	200	2	34	13
Miscanthus	MoO_2/C	MeOH	240	4	26.4	14
Mongolian oak	Ru/WZr	65% MeOH/H_2O (v/v)	250	2	23.6	15
Poplar	Ni-EDTA/Al_2O_3	MeOH	240	3	34.5	16

[a] Yield calculated based on lignin content in each biomass.

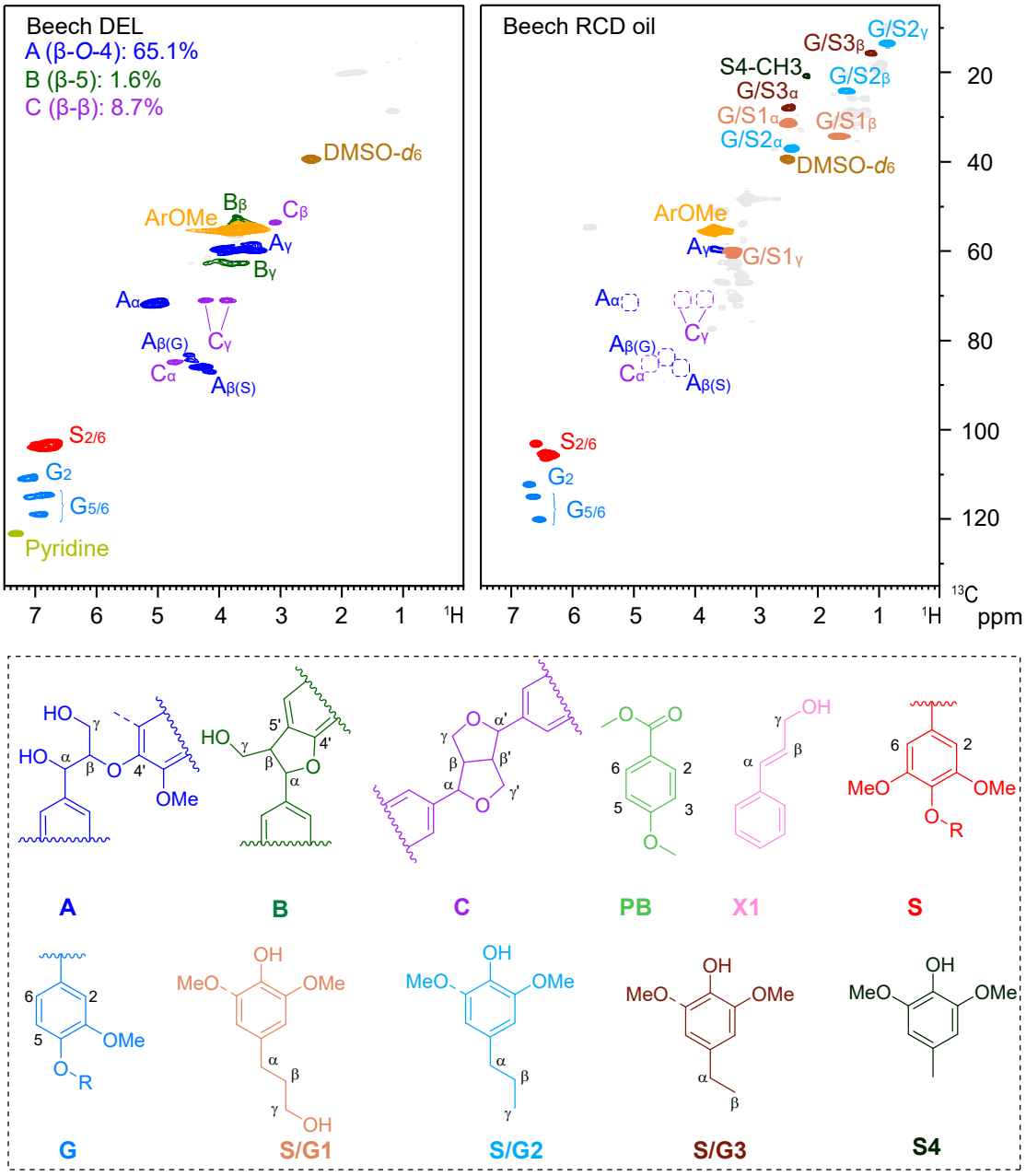

Fig. S28. Total 2D HSQC NMR spectra (δ_C/δ_H 5–135/0–7.5 ppm) for Beech DEL and lignin oil after catalytic hydrogenolysis reaction in DMSO-d_6.

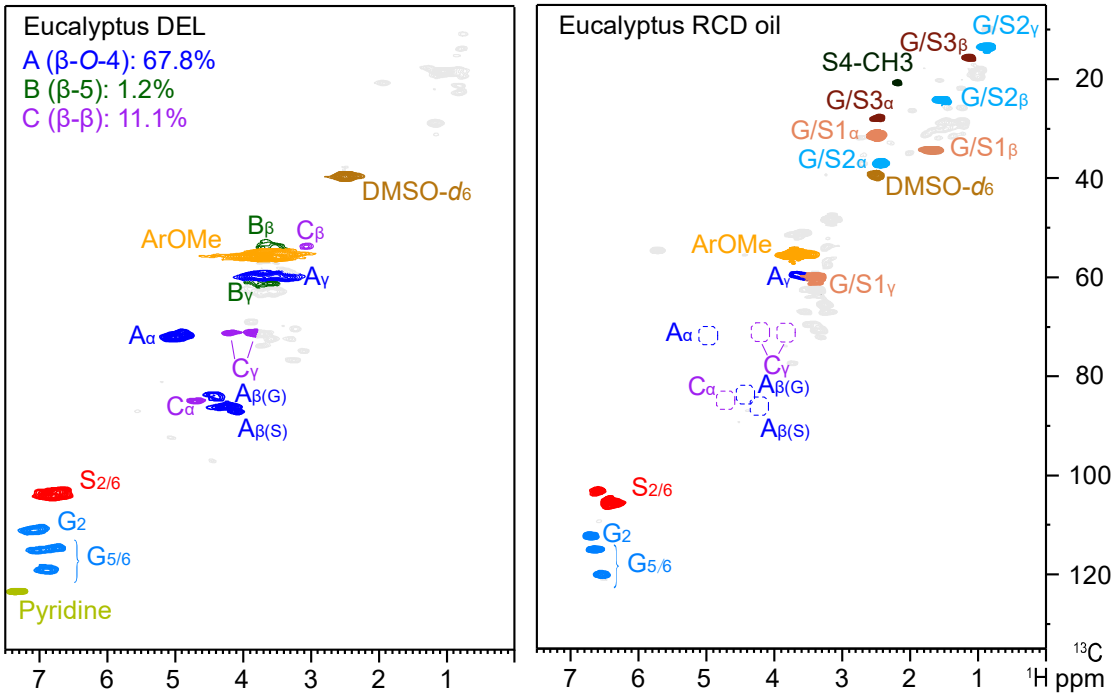

Fig. S29. Total 2D HSQC NMR spectra (δ_C/δ_H 5–135/0–7.5 ppm) for Eucalyptus DEL and lignin oil after catalytic hydrogenolysis reaction in DMSO-d_6.

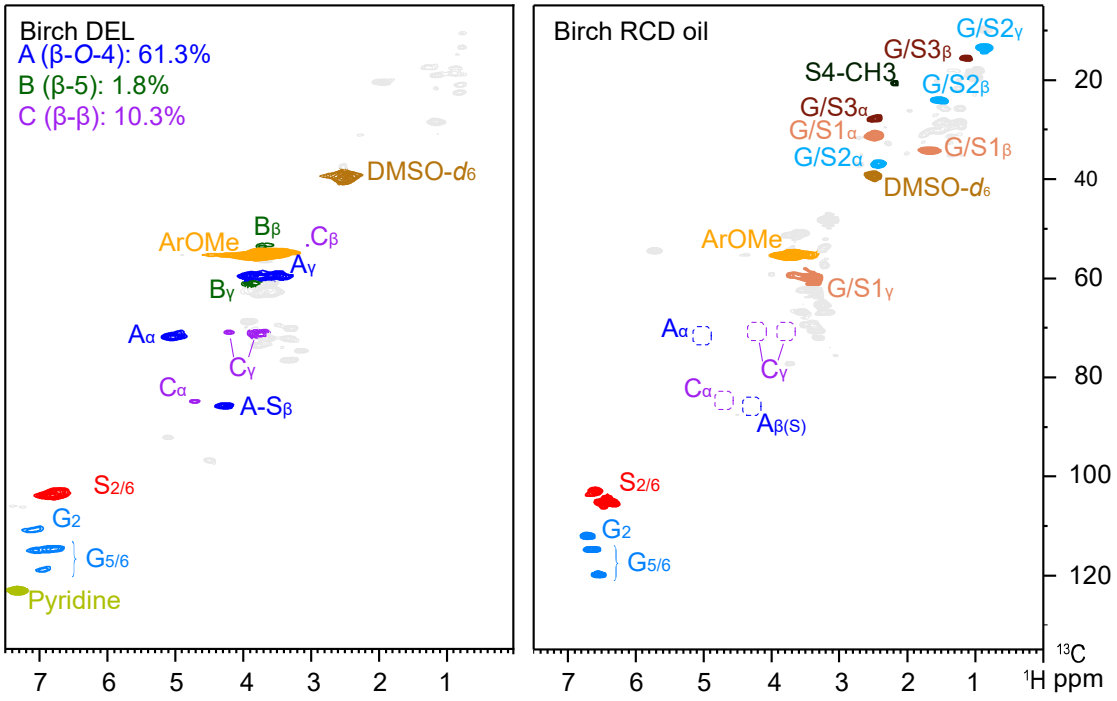

Fig. S30. Total 2D HSQC NMR spectra (δ_C/δ_H 5–135/0–7.5 ppm) for Birch DEL and lignin oil after catalytic hydrogenolysis reaction in DMSO-d_6.

8. Catalyzed hydrogenolysis of β-*O*-4' model compounds with CuO/c-UiO-66

General procedure: In a typical experiment, the substrate (10 mg), CuO/c-UiO-66 (25 mg) and MeOH (10 mL) were combined into a 50 mL stainless autoclave. After flushing with H_2 for three times, the reactor was heated to temperature reflex for 4h with a stirring speed of 800 rpm. After the reaction, the reactor was cooled and carefully depressurized, and the organic products were extracted with dichloromethane and analyzed by GC-FID and GC-MS. The products were identified by comparison with authentic samples.

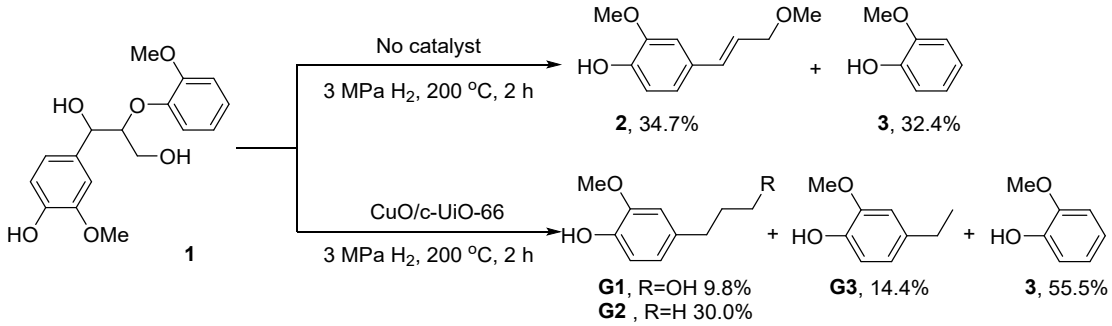

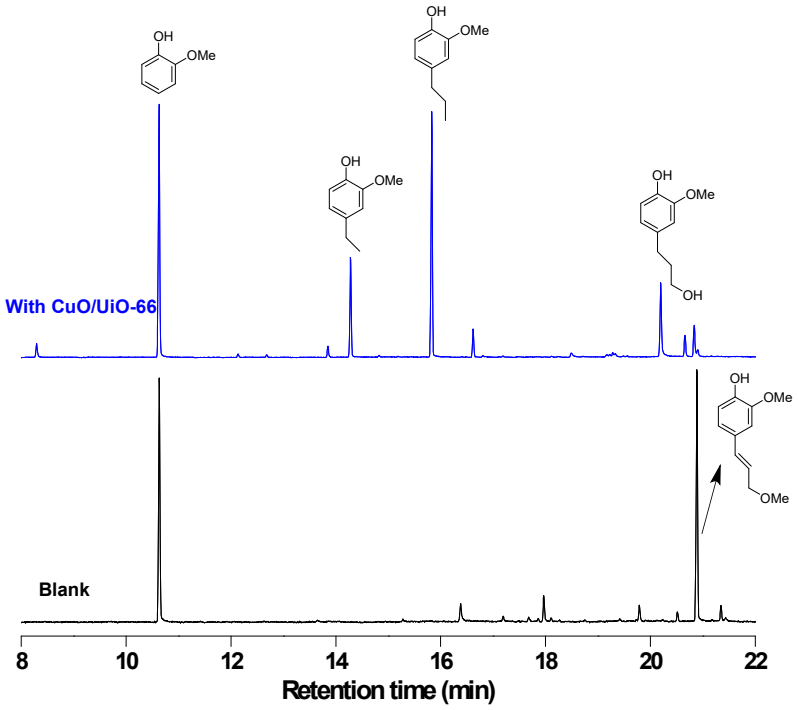

Fig. S31. Catalyzed hydrogenolysis of β-*O*-4' model compound **1** with or without CuO/c-UiO-66.

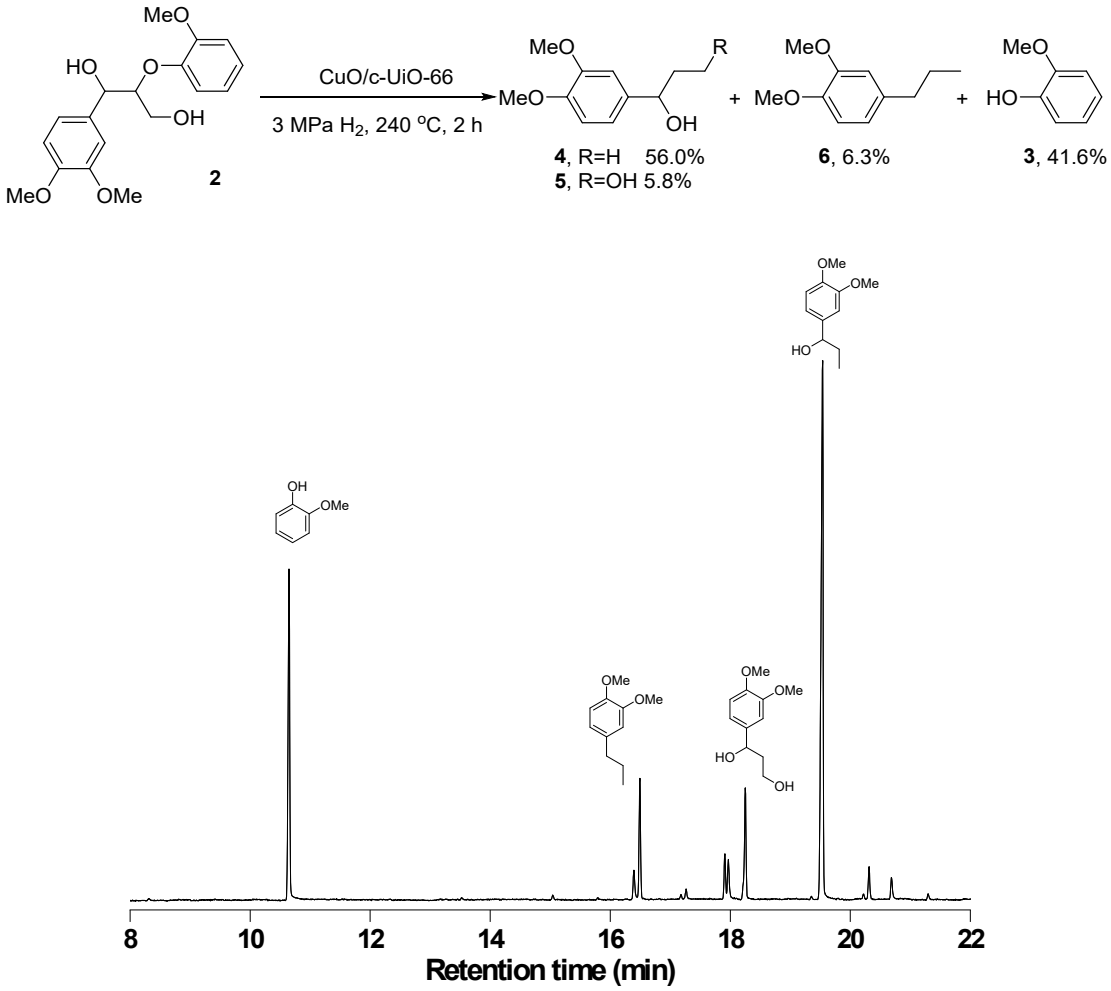

Fig. S32. Catalyzed hydrogenolysis of β-*O*-4' model compound **2** with CuO/c-UiO-66.

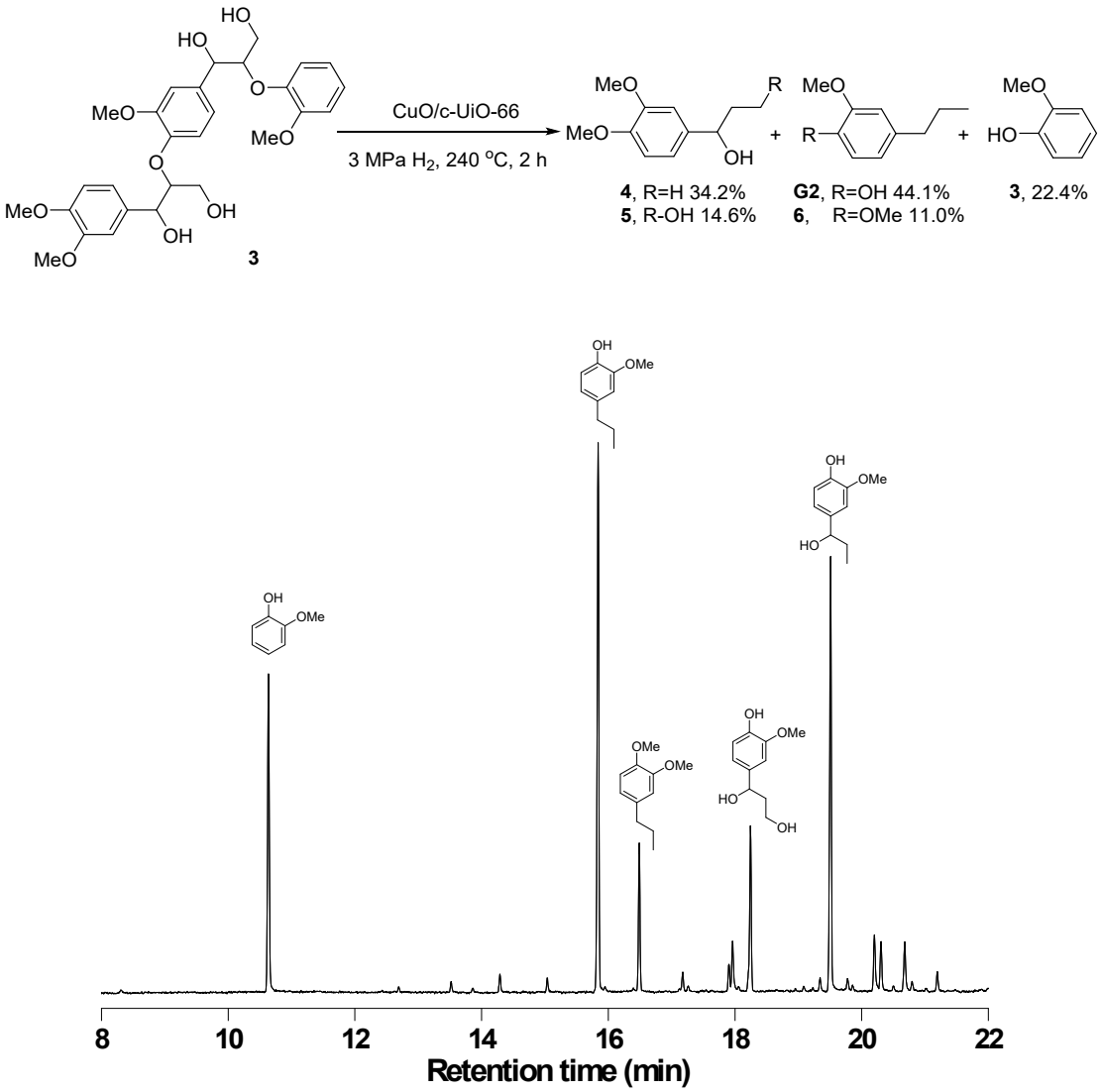

Fig. S33. Catalyzed hydrogenolysis of β-*O*-4' model compound **3** with CuO/c-UiO-66.

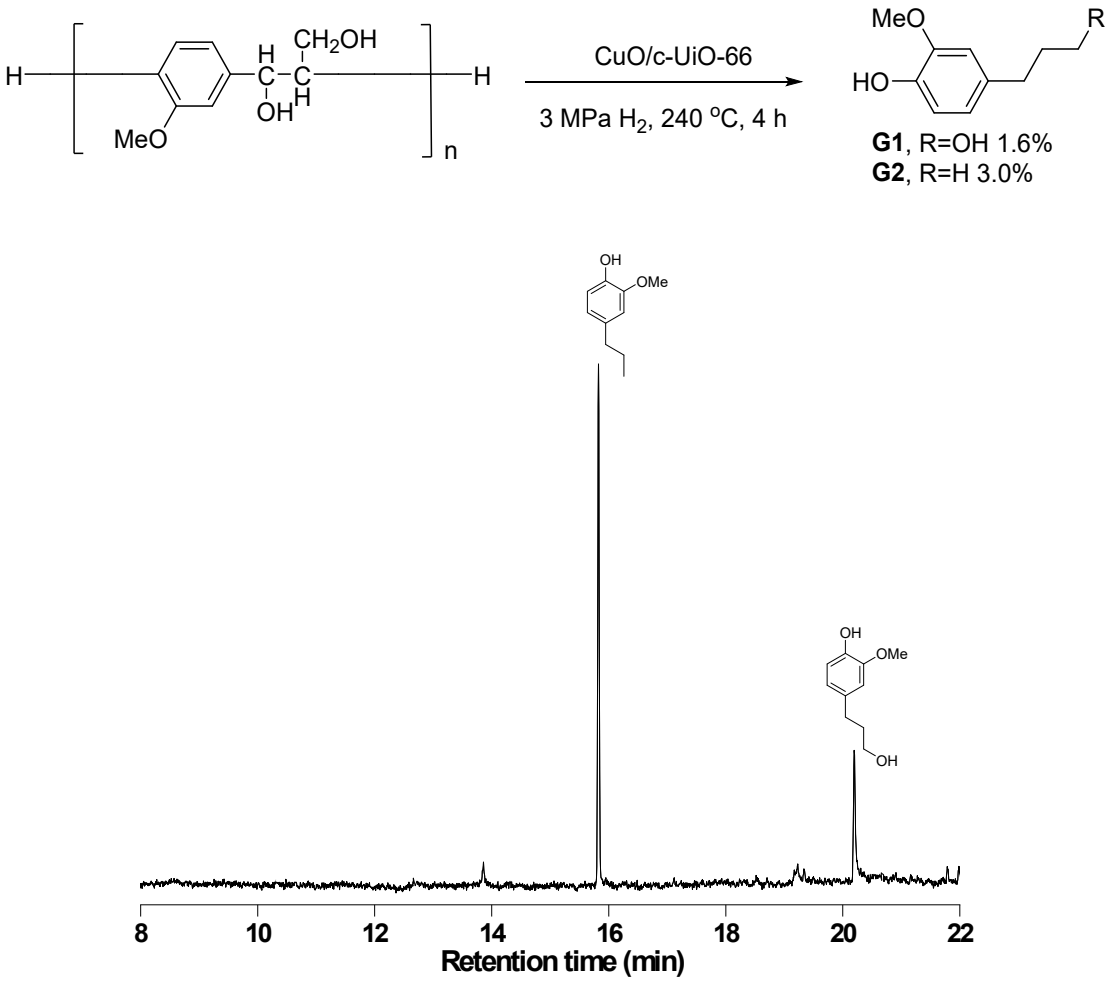

Fig. S34. Catalyzed hydrogenolysis of β-*O*-4' polymer model with CuO/c-UiO-66.

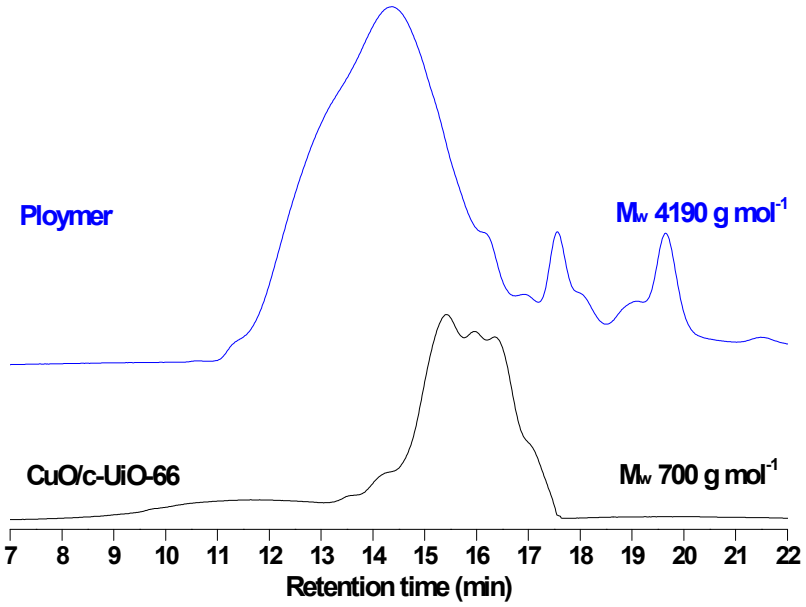

Fig. S35. GPC of β-*O*-4' polymer model and decomposition of polymer oil.

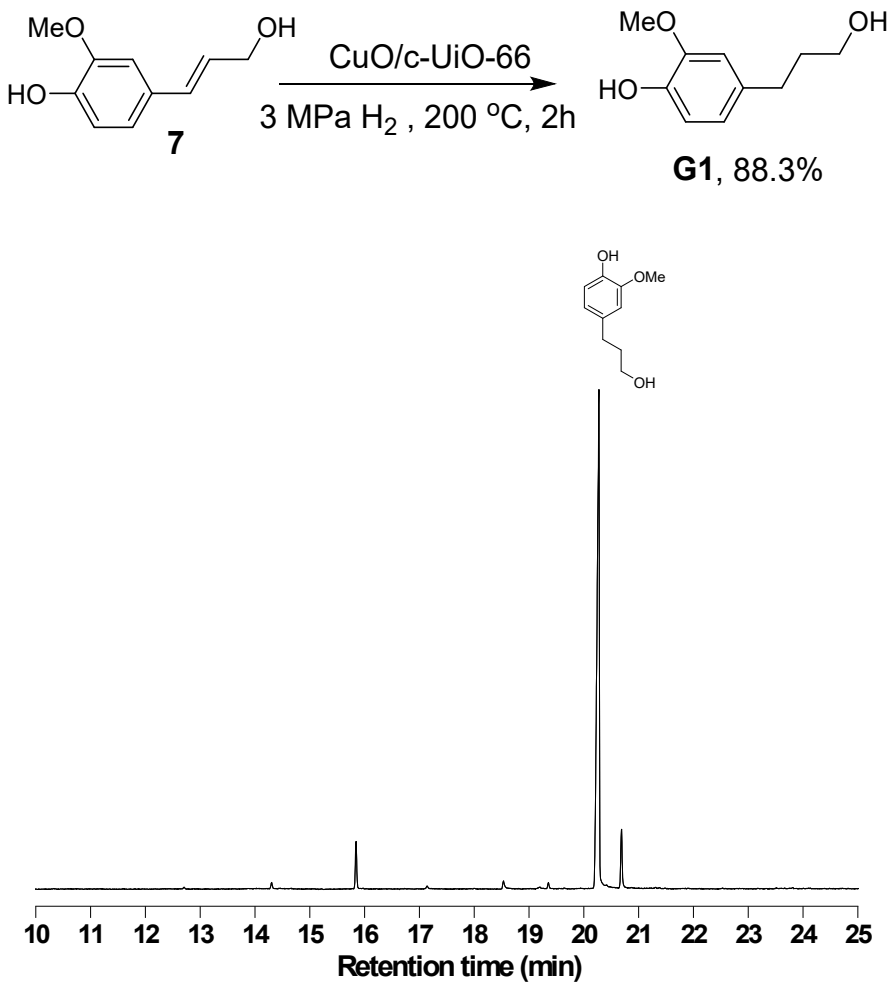

Fig. S36. Catalyzed hydrogenolysis of **7** with CuO/c-UiO-66.

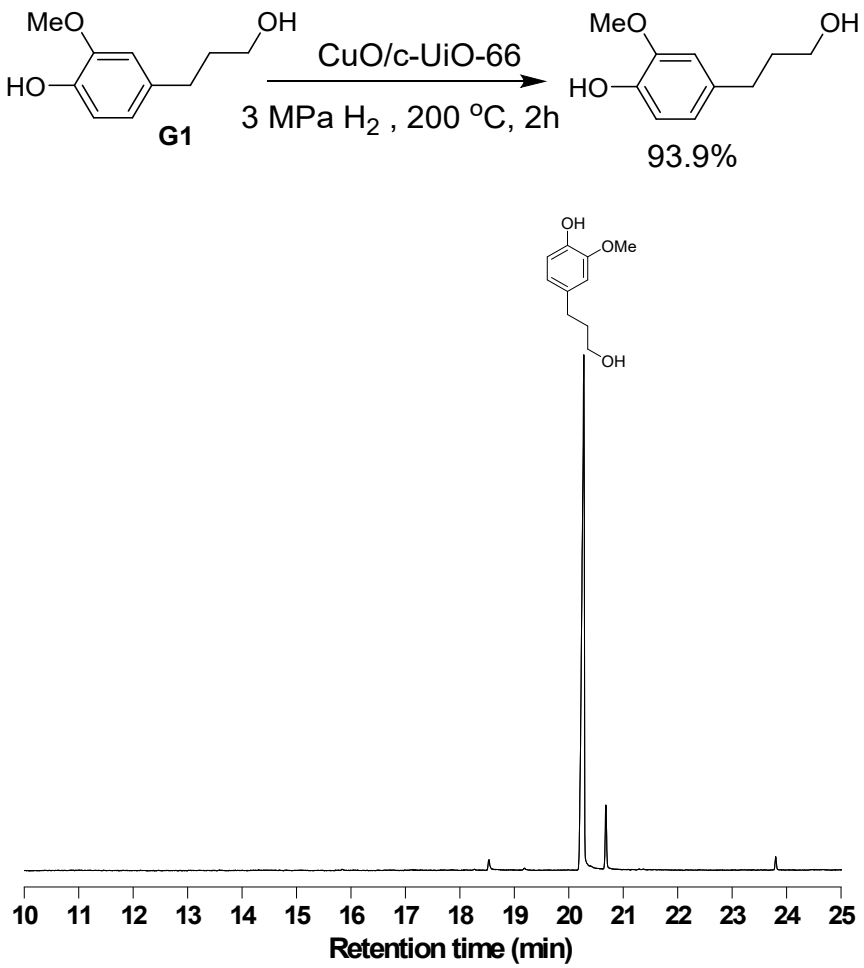

Fig. S37. Catalyzed hydrogenolysis of **G1** with CuO/c-UiO-66.

9. Identification and quantitation of phenolic monomers

More details could be seen in our previous work.[5]

CAS: 6766-82-1, 4-n-propanolsyringol (syringylpropaPne, S1) was prepared following previously reported procedures.[17]

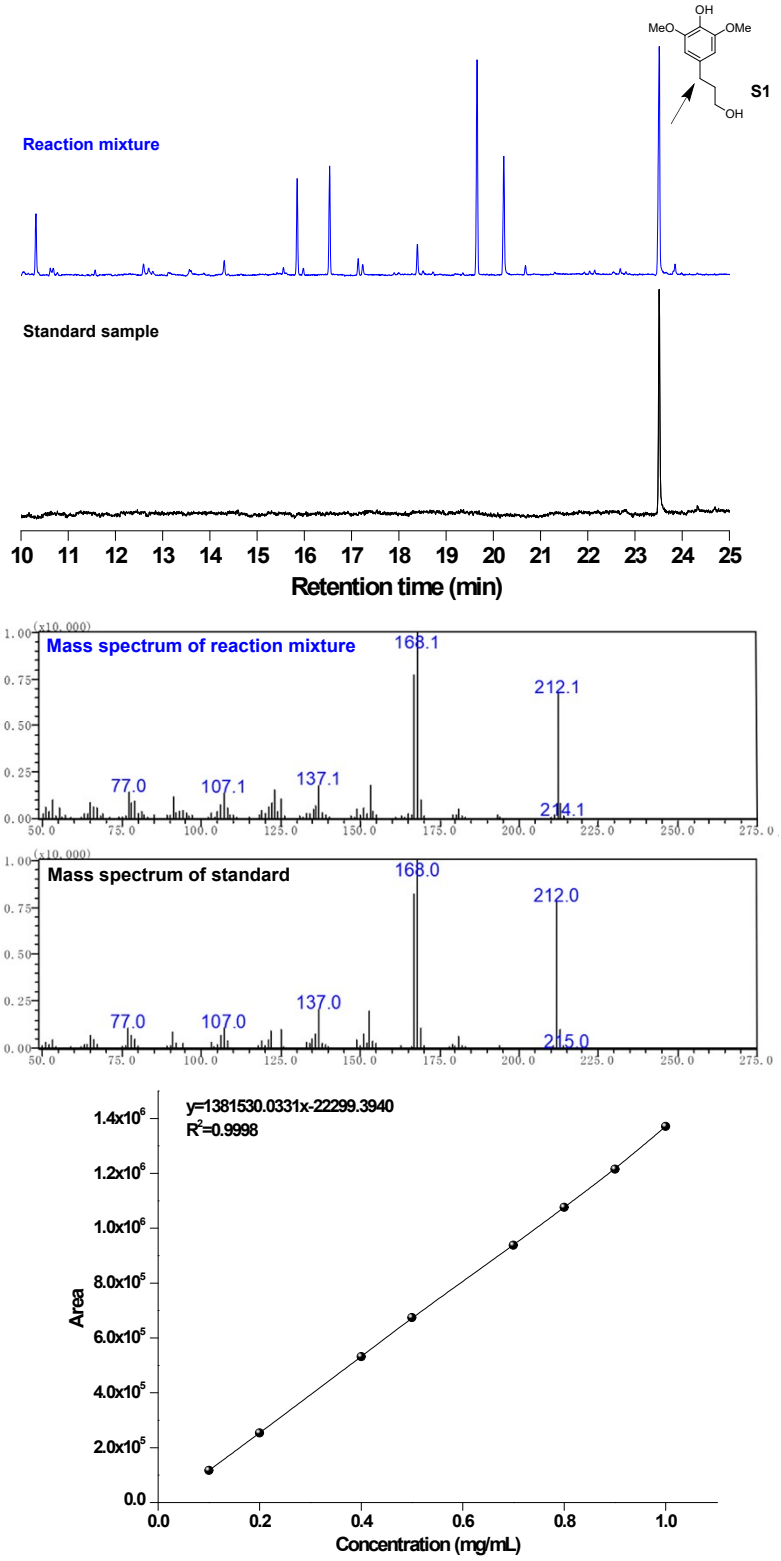

Fig. S38. Standard curve line of 4-n-propanolsyringol (S1).

CAS:20736-25-8, 4-n-propylsyringol (benzenepropanol, S2) was prepared following previously reported procedure.[18]

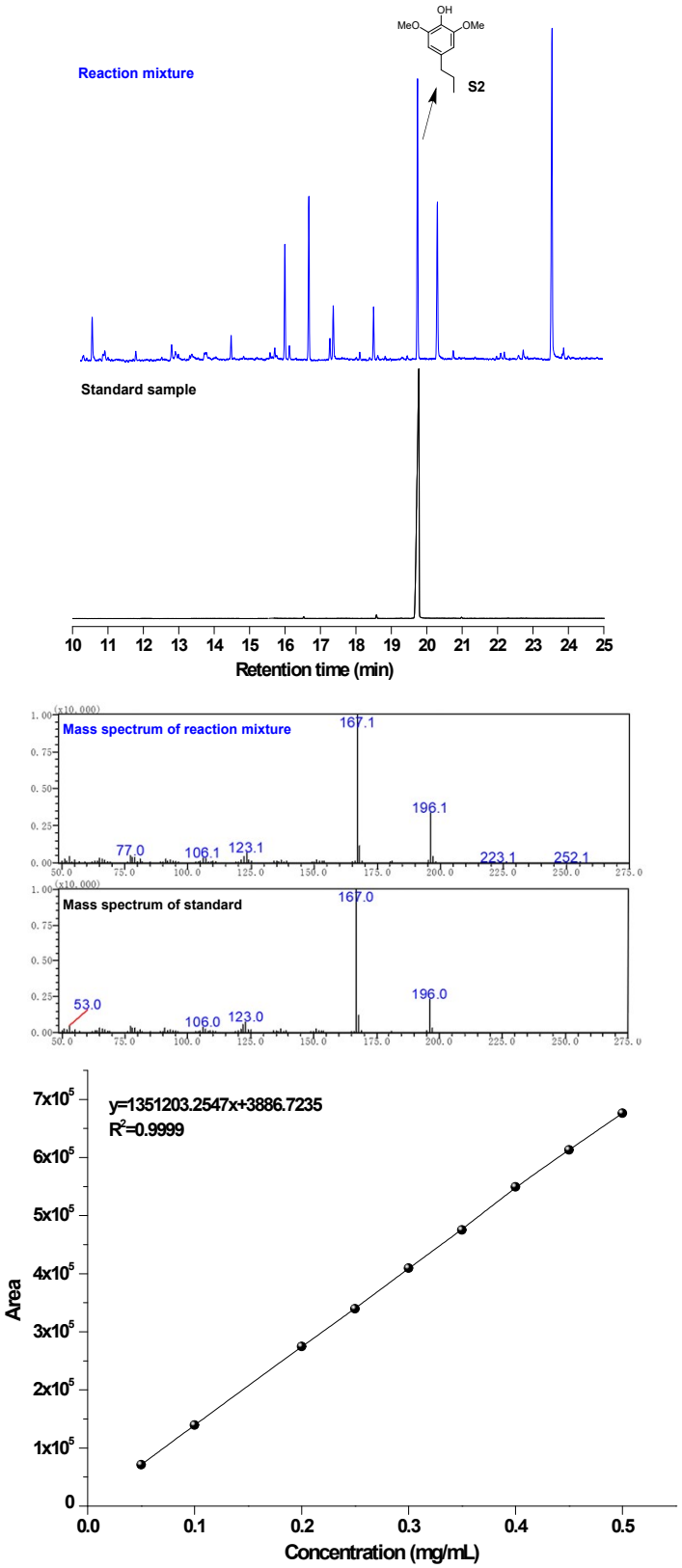

Fig. S39. Standard curve line of 4-n-propylsyringol (S2).

CAS: 2305-13-7, 4-n-guaiacol (dihydroconiferyl alcohol, G1) was prepared following previously reported procedures.[18]

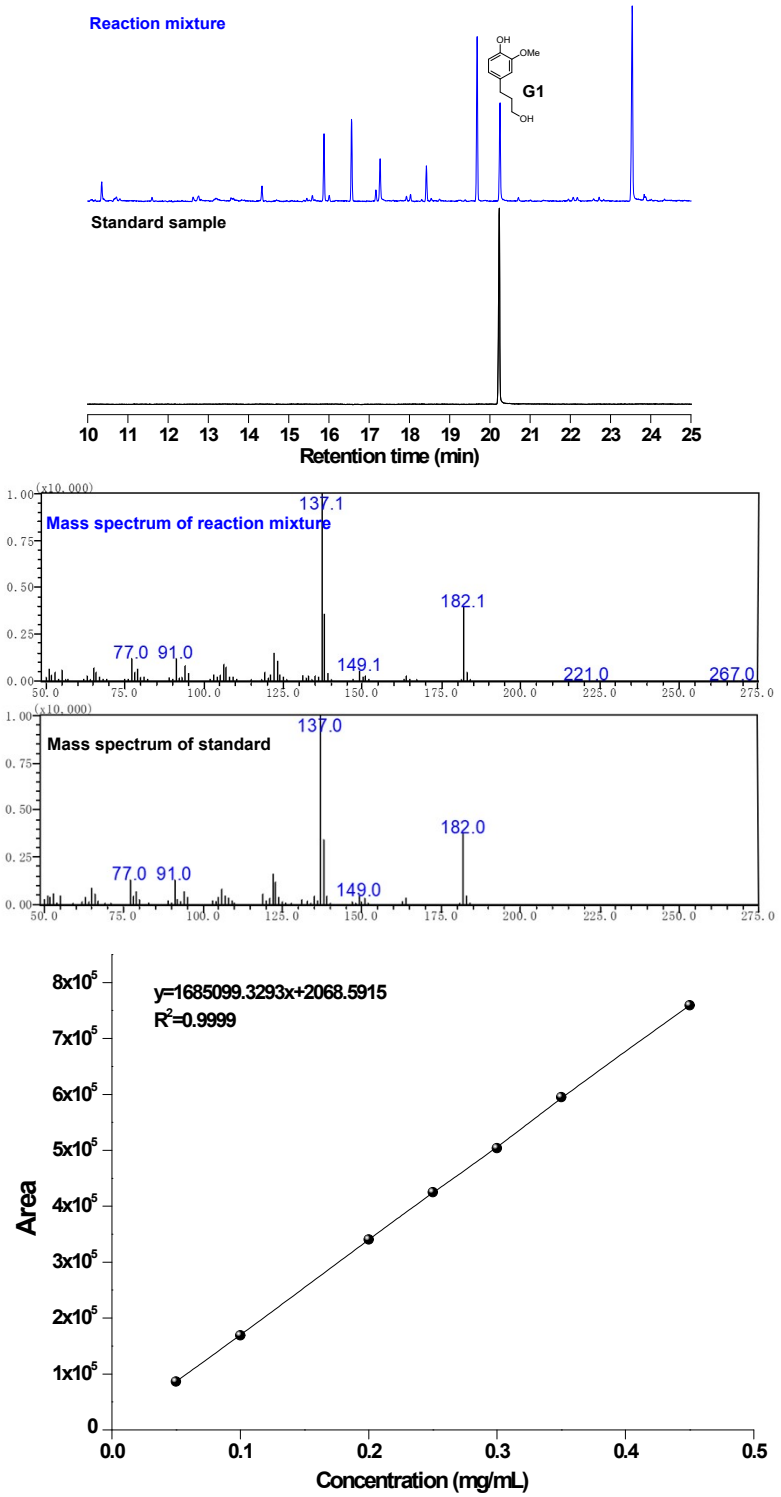

Fig. S40. Standard curve line of 4-n-guaiacol (G1).

CAS: 2785-87-7, 4-n-propylguaiacol (G2) was commercially available.

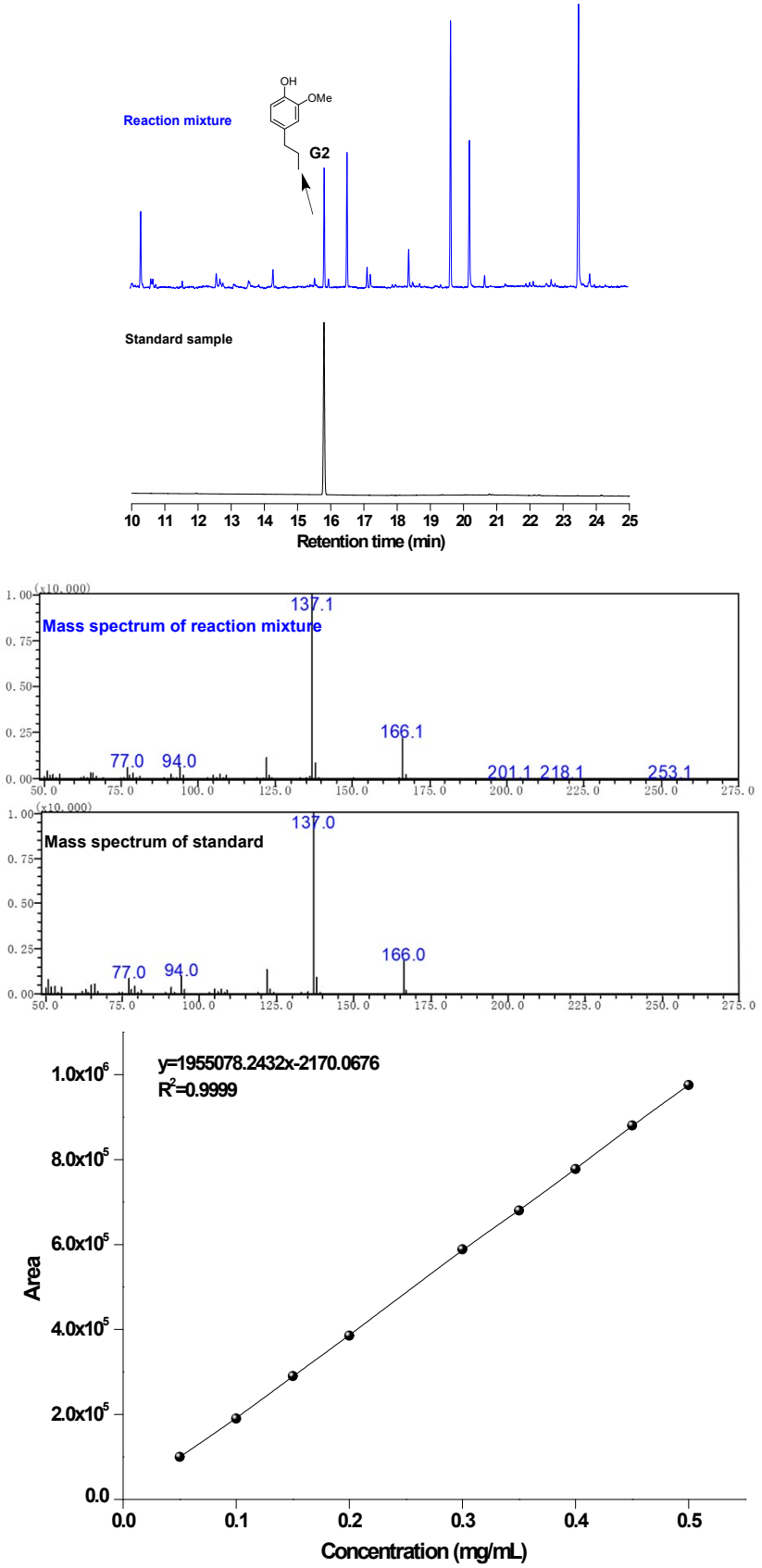

Fig. S41. Standard curve line of 4-n-propylguaiacol (G2).

CAS: 14059-92-8, 2,6-Dimethoxy-4-ethylphenol (S3) was commercially available.

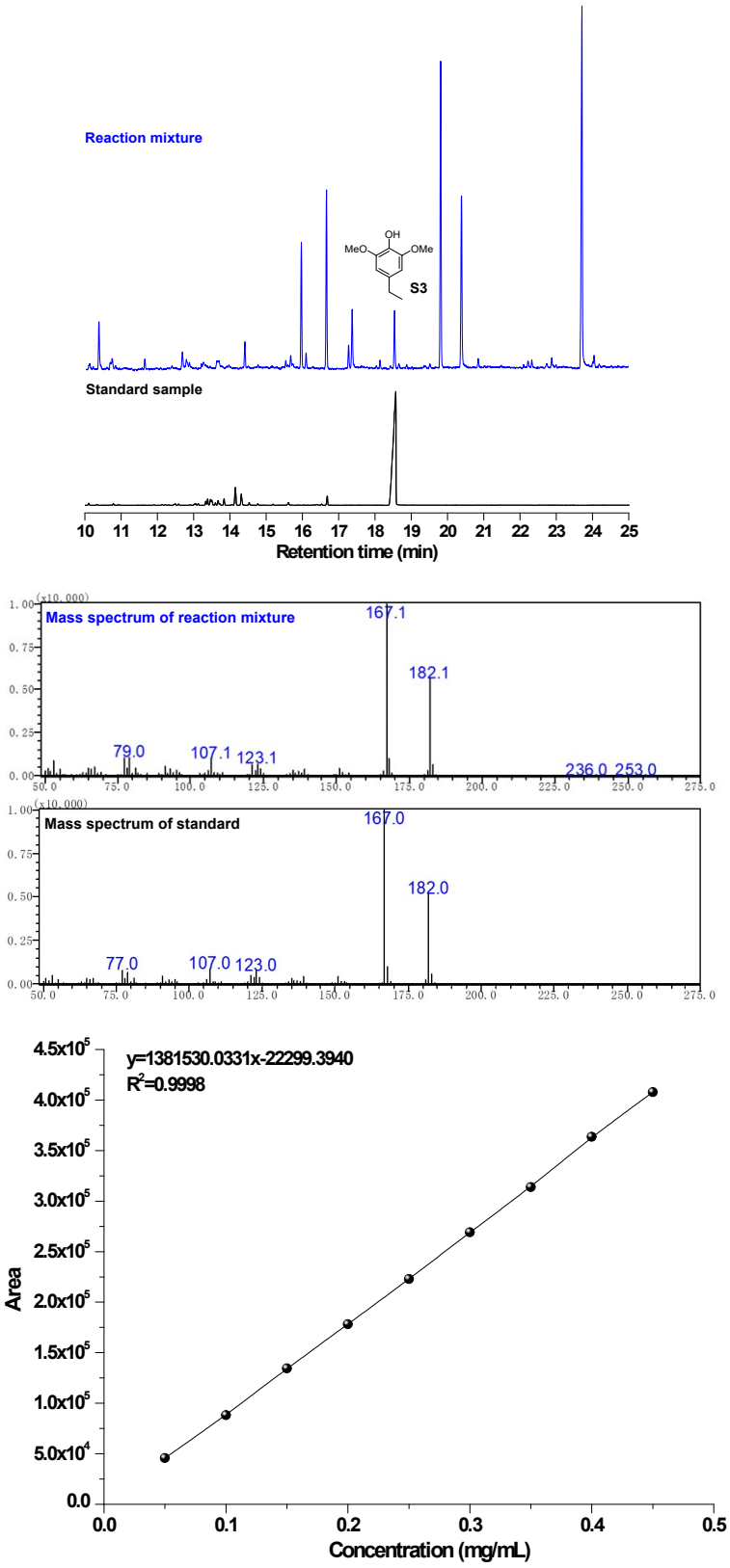

Fig. S42. Standard curve line of 2,6-Dimethoxy-4-ethylphenol (S3).

CAS: 99-76-3, Methyl 4-hydroxybenzoatel (H1) was commercially available.

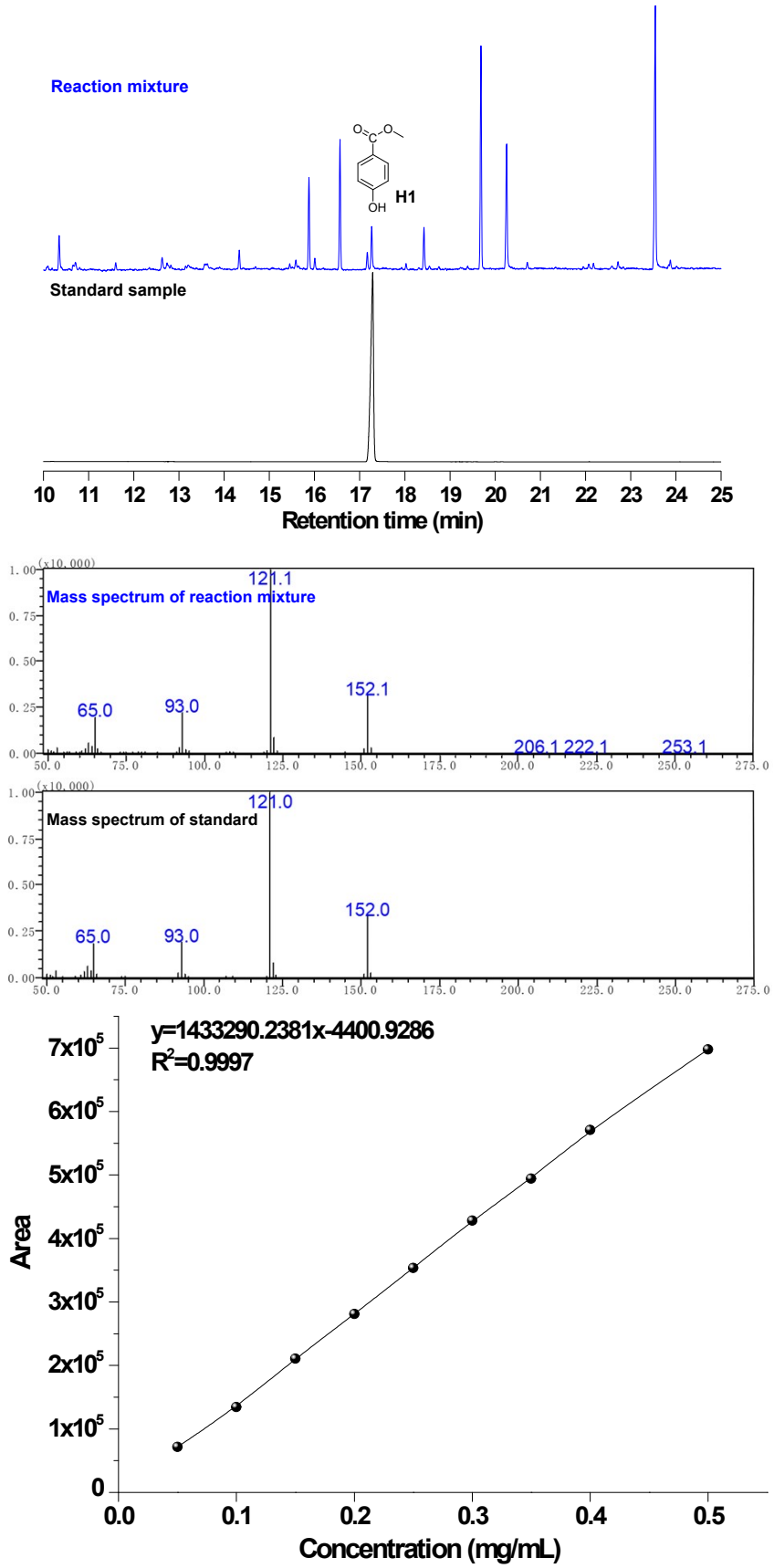

Fig. S43. Standard curve line of Methyl 4-hydroxybenzoatel (H1).

CAS: 106-44-5, 4-methyl phenol (L) was commercially available.

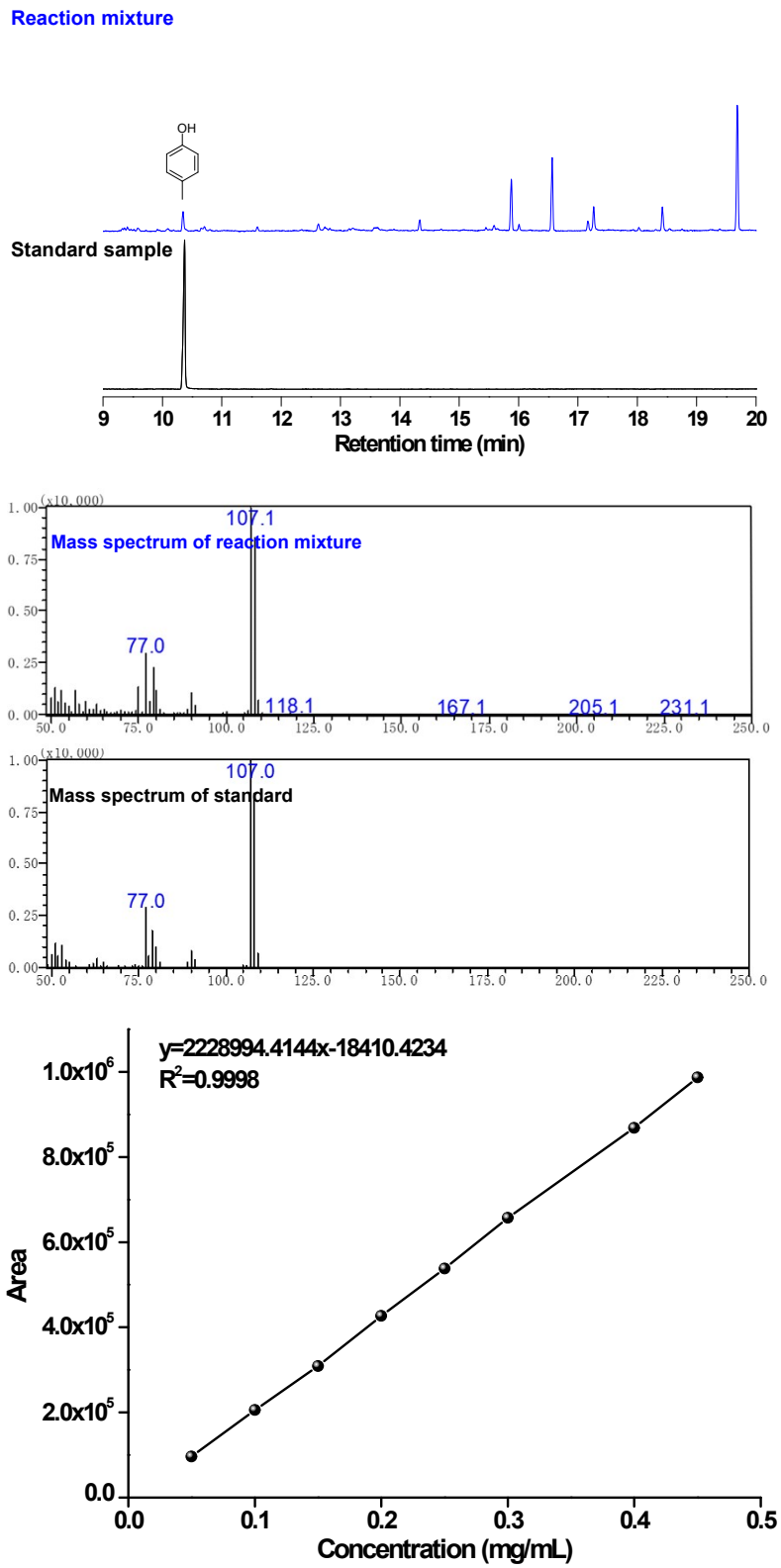

Fig. S44. Standard curve line of 4-methyl phenol (L).

CAS: 6638-05-7, 2,6-Dimethoxy-4-methylphenol (S4) was commercially available.

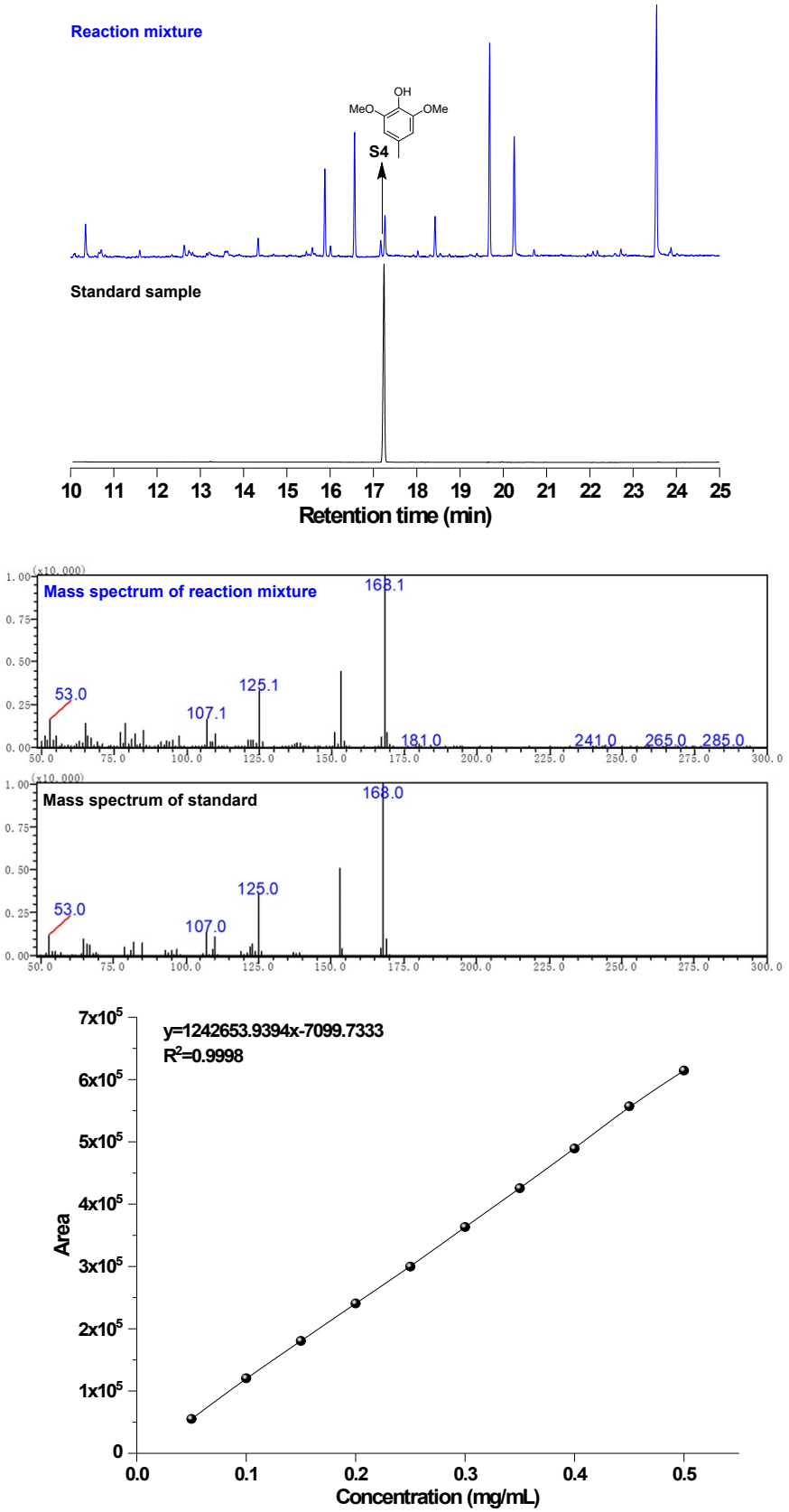

Fig. S45. Standard curve line of 2,6-Dimethoxy-4-methylphenol (S4).

CAS: 2785-89-9, 4-ethylguaiacol (G3) was commercially available.

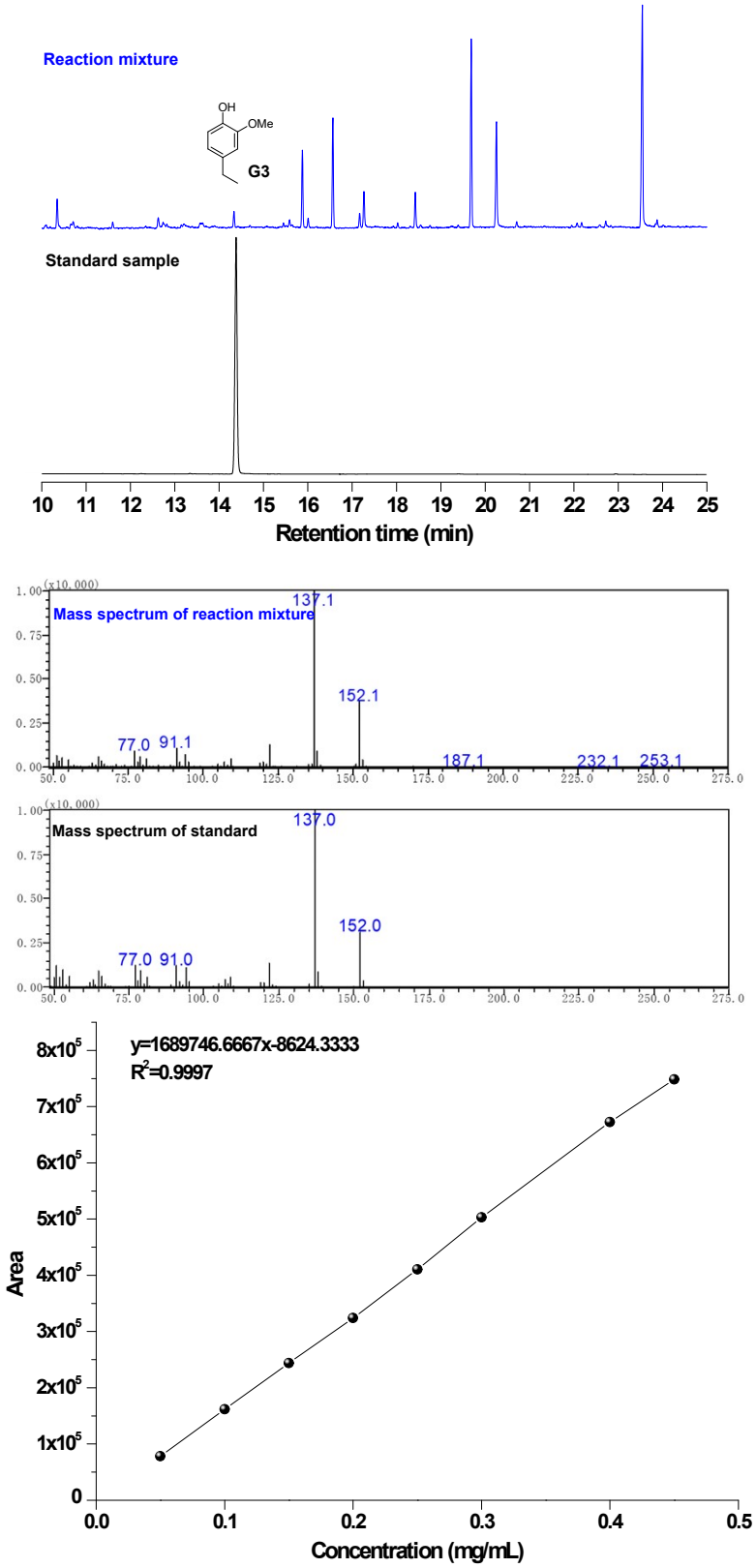

Fig. S46. Standard curve line of 4-ethylguaiacol (G3).

CAS: 63644-71-3, 2-methoxy-4-(3-methoxy-1-propenyl) phenol (2) was commercially available.

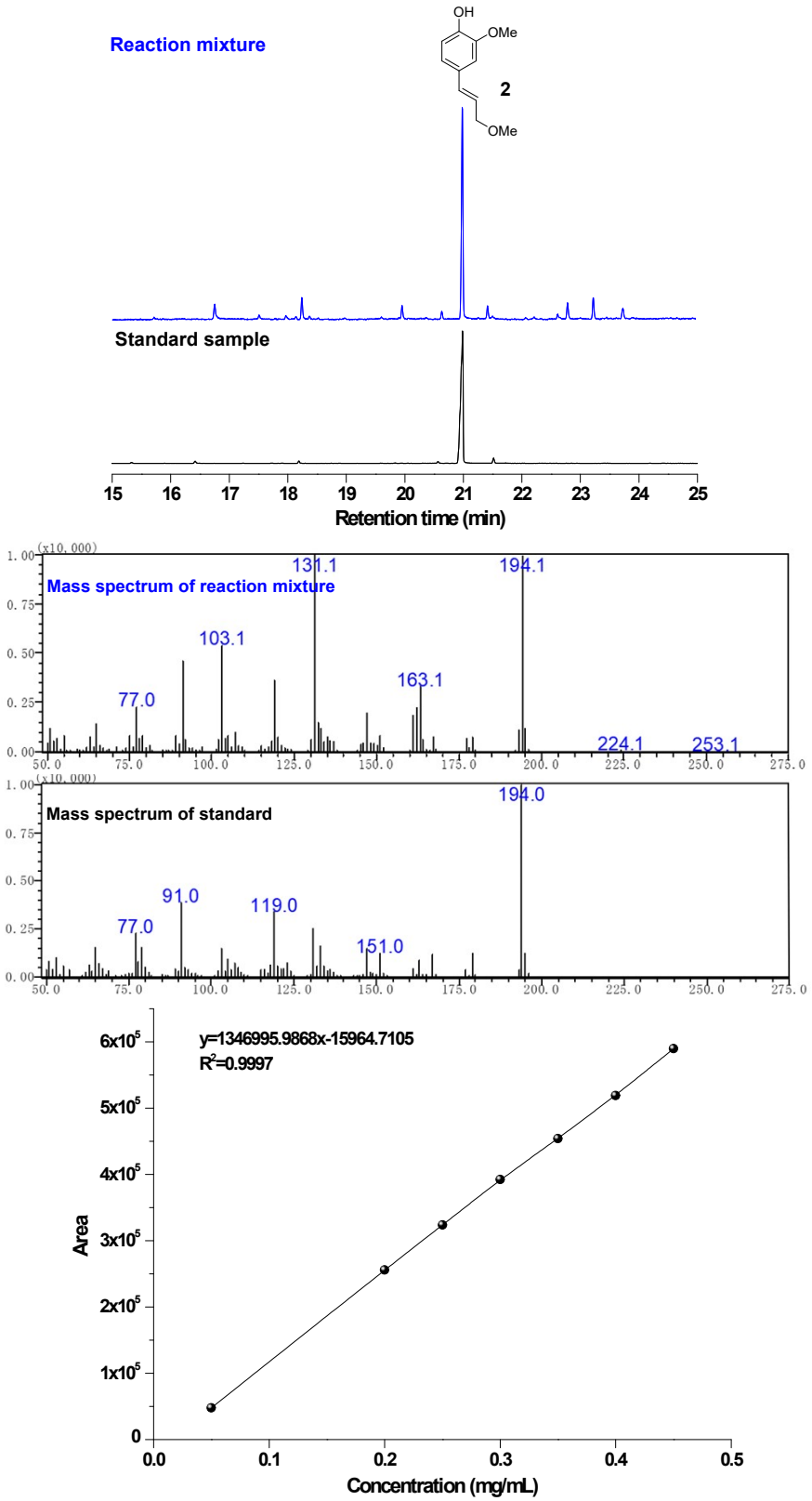

Fig. S47. Standard curve line of 2-methoxy-4-(3-methoxy-1-propenyl) phenol (2).

CAS: 90-05-1, guaiacol (3) was commercially available.

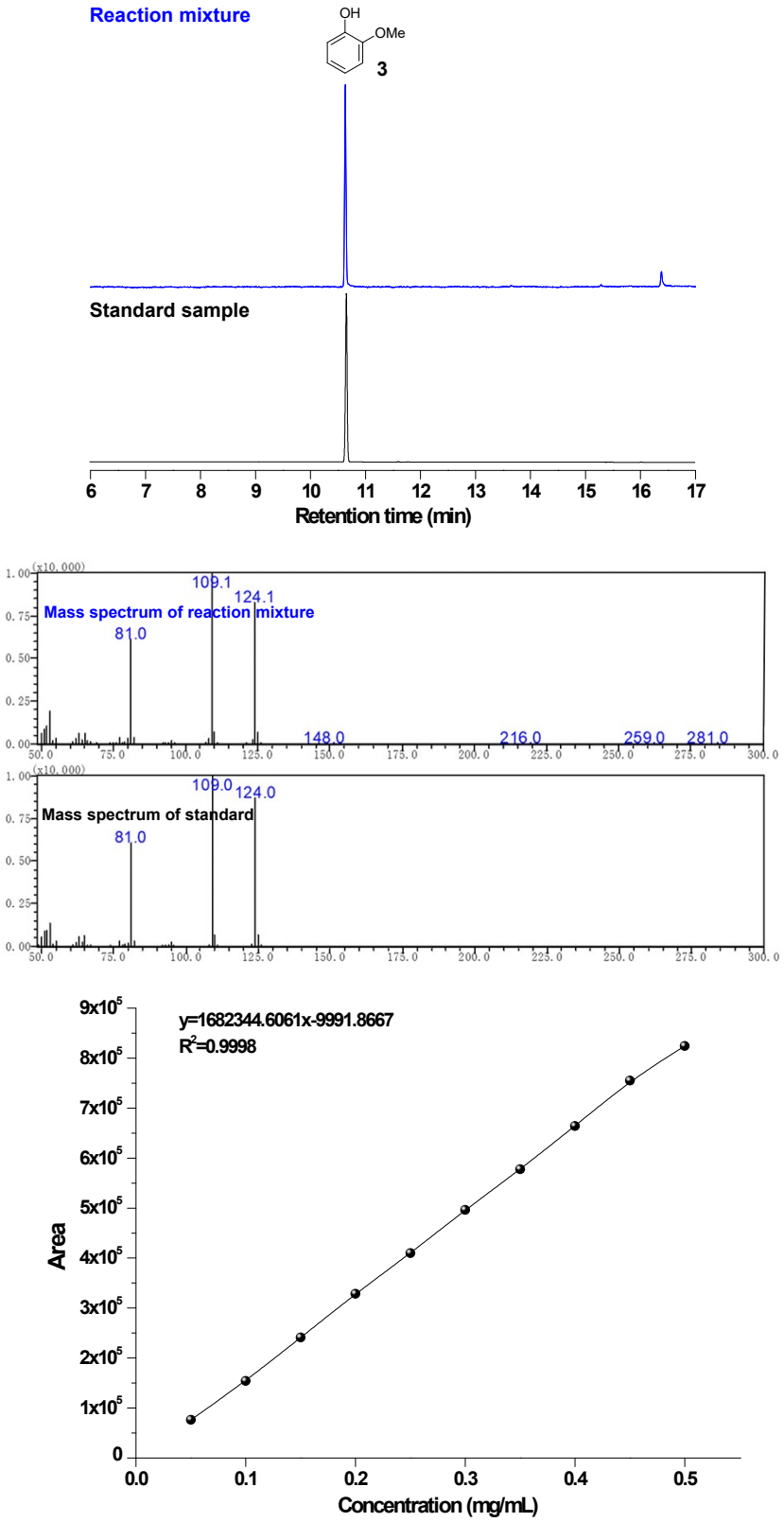

Fig. S48. Standard curve line of guaiacol (3).

CAS: 10548-83-1, 1-(3',4'-dimethoxyphenyl)-1-propanol (4) was commercially available.

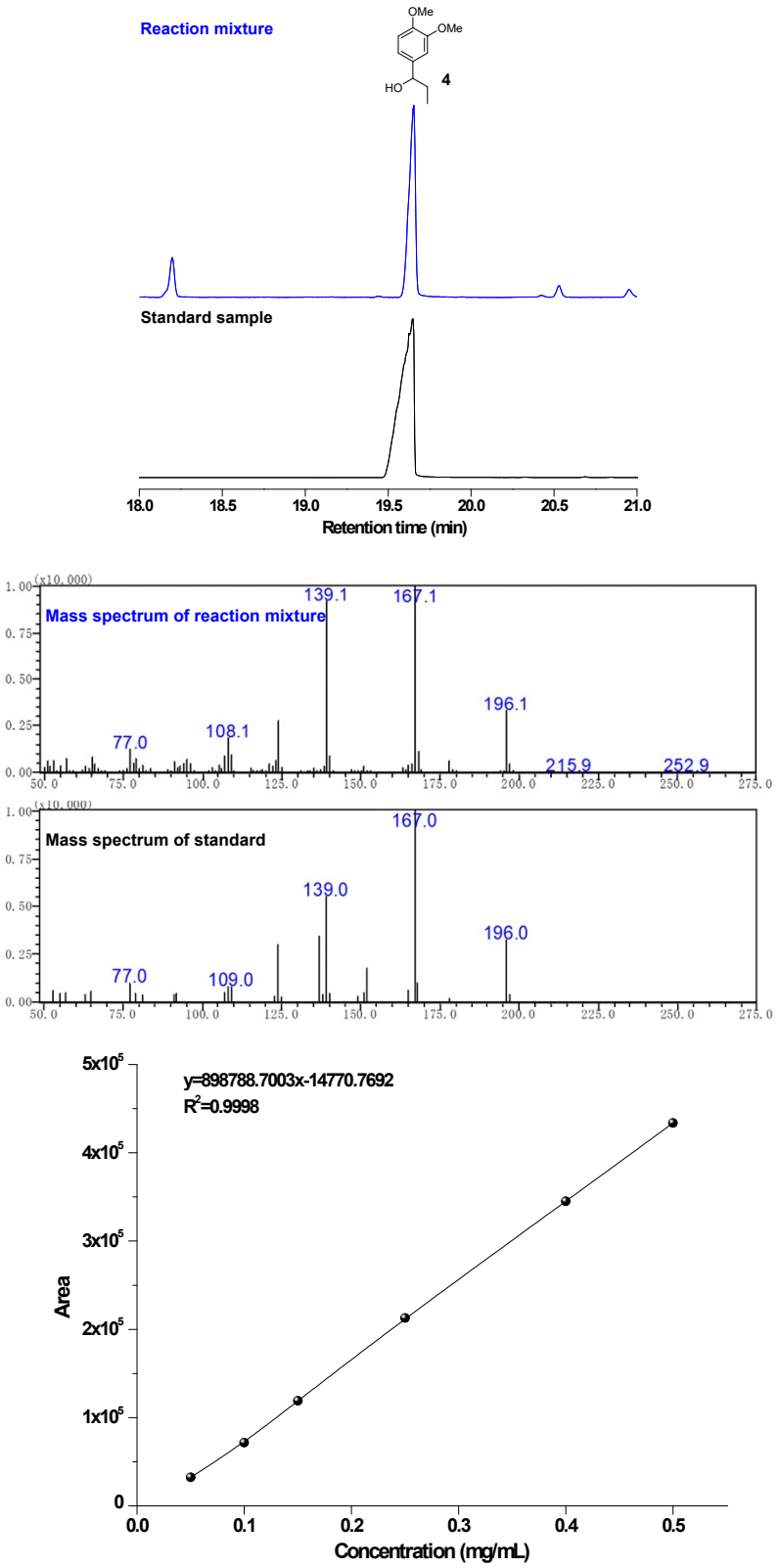

Fig. S49. Standard curve line of 1-(3',4'-Dimethoxyphenyl)-1-propanol (4).

CAS: 5888-52-8, 1,2-dimethoxy-4-n-propylbenzene (6) was commercially available.

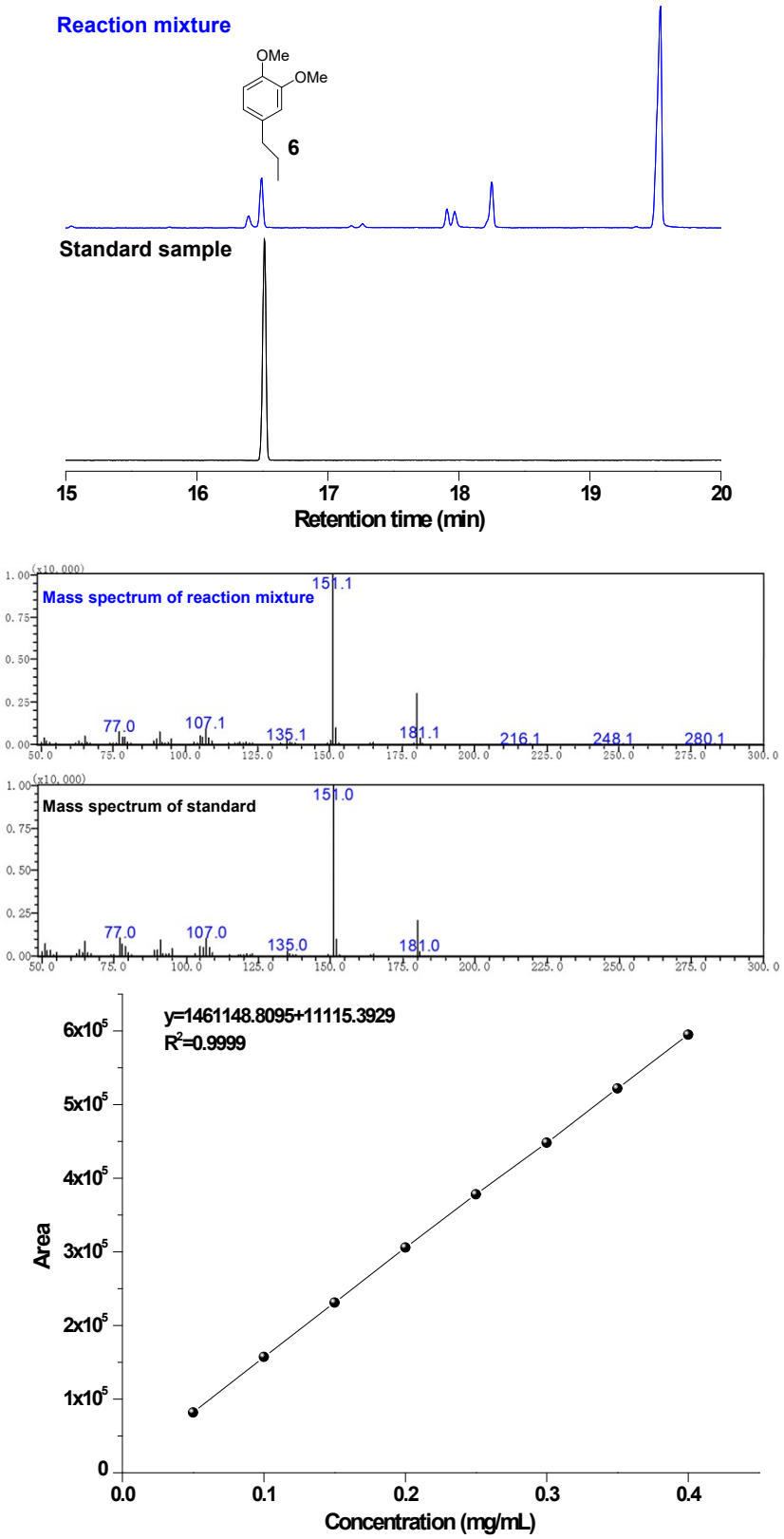

Fig. S50. Standard curve line of 1,2-dimethoxy-4-n-propylbenzene (6).

10. References

1. C.S. Lancefield, L.W. Teunissen, B.M. Weckhuysen, and P.C.A. *Green Chem*., 2018, **20**, 3214-3221.
2. J. Chen, F. Lu, X. Si, X. Nie, J. Chen, R. Lu, and J. Xu, *ChemSusChem*, 2016, **9**, 3353-3360.
3. H. Li, and G. Song, *ACS Catal*., 2020, **10**, 12229-12238.
4. H. Li, and G. Song, *ACS Catal*., 2019, **9**, 4054-4064.
5. Q. Wang, L.-P. Xiao, Y.-H. Lv, W.-Z. Yin, C.-J. Hou, and R.-C. Sun, *ACS Catal*., 2022, **12**, 11899-11909.
6. T. Liu, X. Hong, and G. Liu, *ACS Catal*., 2020, **10**, 93-102.
7. L.-P. Xiao, Z.-J. Shi, F. Xu, and R.-C. Sun, *Bioresour. Technol*., 2013, **135**, 73-81.
8. H.-M. Wang, B. Wang, J.-L. Wen, T.-Q. Yuan, and R.-C. Sun, *ACS Sustainable Chem. Eng*., 2017, **5**, 11618-11627.
9. D.J. McClelland, A.H. Motagamwala, Y. Li, M.R. Rover, A.M. Wittrig, C. Wu, J.S. Buchanan, R.C. Brown, J. Ralph, J.A. Dumesic, and G.W. Huber, *Green Chem*., 2017, **19**, 1378-1389.
10. S. Van den Bosch, T. Renders, S. Kennis, S.F. Koelewijn, G. Van den Bossche, T. Vangeel, A. Deneyer, D. Depuydt, C.M. Courtin, J.M. Thevelein, W. Schutyser, and B.F. Sels, *Green Chem*., 2017, **19**, 3313-3326.
11. Z. Sun, G. Bottari, A. Afanasenko, M.C.A. Stuart, P.J. Deuss, B. Fridrich, and K. Barta, *Nat. Catal.*, 2018, **1**, 82-92.
12. J. Sun, H. Li, L.-P. Xiao, X. Guo, Y. Fang, R.-C. Sun, and G. Song, *ACS Sustainable Chem. Eng.*, 2019, **7**, 4666-4674.
13. S. Rautiainen, D. Di Francesco, S.N. Katea, G. Westin, D.N. Tungasmita, and J.S.M. Samec, *ChemSusChem*, 2019, **12**, 404-408.
14. X. Gong, J. Sun, X. Xu, B. Wang, H. Li, and F. Peng, *Bioresour. Technol*., 2021, **333**, 124977.
15. S. Oh, S. Gu, J.-W. Choi, D.J. Suh, H. Lee, C.S. Kim, K.H. Kim, C.-J. Yoo, J. Choi, and J.-M. Ha, *J. Environ. Chem. Eng*., 2022, **10**, 108085.
16. M. Hou, H. Chen, Y. Li, H. Wang, L. Zhang, and Y. Bi, *Energy Fuels*, 2022, **36**, 1929-1938.
17. I. Kumaniaev, E. Subbotina, J. Sävmarker, M. Larhed, M.V. Galkin, and J.S.M. Samec, *Green Chem*., 2017, **19**, 5767-5771.
18. N. Daubresse, C. Francesch, F. Mhamdi, and C. Rolando, *Synthesis*, 1994, **1994**, 369-371.